

Accepted Manuscript

Design, synthesis, *in vitro* and *in silico* evaluation of a new series of oxadiazole-based anticancer agents as potential Akt and FAK inhibitors

Mehlika Dilek Altıntop, Belgin Sever, Gülşen Akalın Çiftçi, Gülhan Turan-Zitouni, Zafer Asım Kaplancıklı, Ahmet Özdemir



PII: S0223-5234(18)30540-3

DOI: [10.1016/j.ejmech.2018.06.049](https://doi.org/10.1016/j.ejmech.2018.06.049)

Reference: EJMECH 10519

To appear in: *European Journal of Medicinal Chemistry*

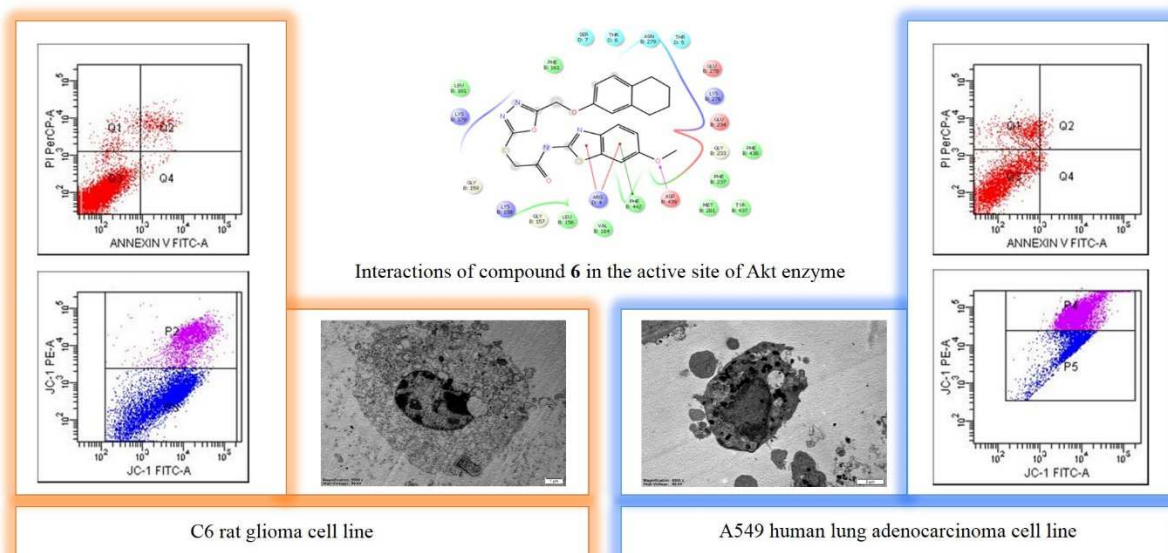
Received Date: 13 April 2018

Revised Date: 19 June 2018

Accepted Date: 21 June 2018

Please cite this article as: M.D. Altıntop, B. Sever, Güş.Akalı. Çiftçi, Gü. Turan-Zitouni, Zafer.Ası. Kaplancıklı, A. Özdemir, Design, synthesis, *in vitro* and *in silico* evaluation of a new series of oxadiazole-based anticancer agents as potential Akt and FAK inhibitors, *European Journal of Medicinal Chemistry* (2018), doi: 10.1016/j.ejmech.2018.06.049.

This is a PDF file of an unedited manuscript that has been accepted for publication. As a service to our customers we are providing this early version of the manuscript. The manuscript will undergo copyediting, typesetting, and review of the resulting proof before it is published in its final form. Please note that during the production process errors may be discovered which could affect the content, and all legal disclaimers that apply to the journal pertain.



C6 rat glioma cell line

A549 human lung adenocarcinoma cell line

Design, synthesis, *in vitro* and *in silico* evaluation of a new series of oxadiazole-based anticancer agents as potential Akt and FAK inhibitors

Mehlika Dilek Altıntop ^{a,*}, Belgin Sever ^a, Gülşen Akalın Çiftçi ^b, Gülhan Turan-Zitouni ^a, Zafer Asım Kaplancıklı ^a, Ahmet Özdemir ^a

^a *Department of Pharmaceutical Chemistry, Faculty of Pharmacy, Anadolu University, 26470 Eskişehir, Turkey*

^b *Department of Biochemistry, Faculty of Pharmacy, Anadolu University, 26470 Eskişehir, Turkey*

* Corresponding author.

E-mail address: mdaltintop@anadolu.edu.tr (M.D. Altıntop).

ABSTRACT

In the current work, new 1,3,4-oxadiazole derivatives were synthesized and investigated for their cytotoxic effects on A549 human lung adenocarcinoma, C6 rat glioma and NIH/3T3 mouse embryonic fibroblast cell lines. Compounds **2**, **6** and **9** were found to be the most potent anticancer agents against A549 and C6 cell lines and therefore their effects on apoptosis, caspase-3 activation, Akt, FAK, mitochondrial membrane potential and ultrastructural morphological changes were evaluated. *N*-(5-Nitrothiazol-2-yl)-2-[[5-[[((5,6,7,8-tetrahydronaphthalen-2-yl)oxy)methyl]-1,3,4-oxadiazol-2-yl]thio]acetamide (**9**) increased early and late apoptotic cell population in A549 and C6 cells more than cisplatin and caused more mitochondrial membrane depolarization in both cell lines than cisplatin. On the other hand, *N*-(6-methoxybenzothiazol-2-yl)-2-[[5-[[((5,6,7,8-tetrahydronaphthalen-2-yl)oxy)methyl]-1,3,4-oxadiazol-2-yl]thio]acetamide (**6**) caused higher caspase-3 activation than cisplatin in both cell lines. Compound **6** showed significant Akt inhibitory activity in both cell lines. Moreover, compound **6** significantly inhibited FAK (Phospho-Tyr397) activity in C6 cell line. Molecular docking simulations demonstrated that compound **6** fitted into the active sites of Akt and FAK with high affinity and substrate-specific interactions. Furthermore, compounds **2**, **6** and **9** caused apoptotic morphological changes in both cell lines obtained from micrographs by transmission electron microscopy. A computational study for the prediction of ADME properties of all compounds was also performed. These compounds did not violate Lipinski's rule, making them potential orally bioavailable anticancer agents.

Keywords: Apoptosis, Akt, Benzothiazole, Cancer, FAK, Oxadiazole, Thiazole.

1. Introduction

Cancer is one of the most formidable afflictions throughout the world [1,2]. By 2030, the annual number of new cancer diagnoses is projected to be 21 million worldwide, with 17 million patients dying of cancer every year and 75 million people living with cancer diagnoses [3].

Over the years, the design of chemotherapy has become increasingly sophisticated due to resistance to existing anticancer drugs and lack of selectivity towards tumor cells [4-6]. In an attempt to enhance efficacy and selectivity, targeted cancer therapies are designed to inhibit the growth, progression, and spread of cancer by interfering with specific molecular targets [7].

Akt pathway is one of the most frequently deregulated signaling pathways in human cancers. Akt, also known as protein kinase B (PKB), is overexpressed or activated in a variety of human cancers, including gliomas, lung, breast, ovarian, gastric and pancreatic carcinomas. Inhibition of Akt signaling results in induction of apoptosis and inhibition of tumor growth. As a result, inhibition of Akt has long been an attractive therapeutic approach in oncology and extensive efforts have been devoted to the discovery of new potent and selective anticancer drugs targeting Akt [7-11]. On the other hand, focal adhesion kinase (FAK, also known as PTK2) has been recognised as a key regulator of growth factor receptor- and integrin-mediated signals governing fundamental processes in healthy and cancer cells. FAK is activated and/or overexpressed in a variety of human cancers, and promotes tumor progression and metastasis. For this reason, FAK has emerged as an outstanding therapeutic target for cancer, and several FAK inhibitors have been developed and are being tested in clinical phase trials [12-16].

In the last few decades, oxadiazoles have been the subject of considerable research owing to their metabolic profile and ability to engage in hydrogen bonding with receptor site. Moreover, oxadiazoles have been frequently used in drug-like molecules as bioisosters of esters and amides [17,18]. Recent studies have pointed out the importance of oxadiazole scaffold in the field of cancer research. 1,3,4-Oxadiazole derivatives have been reported to show potent antitumor activity against different cancer cell lines through the inhibition of different enzymes and growth factors including focal adhesion kinase (FAK), telomerase, histone deacetylase (HDAC), methionine aminopeptidase (MetAP), thymidylate synthase (TS), glycogen synthase kinase-3 (GSK), epidermal growth factor (EGF) and vascular endothelial growth factor (VEGF). Among these derivatives, zibotentan is an anticancer drug

candidate in late stage clinical trials (Fig. 1). Due to the significant medicinal importance of oxadiazoles as anticancer agents, oxadiazole has emerged as a promising lead structure for the generation of new active anticancer agents and in the process of anticancer drug development [19,20]. On the other hand, the myriad spectrum of therapeutic applications associated with thiazoles and benzothiazoles has encouraged medicinal chemists to synthesize a large number of new therapeutic agents [21-30]. In particular, the clinical efficacy of tiazofurin, bleomycins (BLMs) and dasatinib (Fig. 2) has pointed out the medicinal significance of thiazole scaffold in the field of current cancer research [21-25]. Recent patents have indicated that thiazole derivatives show potent antitumor activity against different cancer cell lines through the inhibition of kinases, pro-matrix metalloproteinase activation, signal transducer and activator of transcription 3 (STAT3), Bcl-2 family, HDACs [23]. In recent years, benzothiazole has emerged as a privileged scaffold for anticancer drug discovery. Therefore, antitumor effects of benzothiazole derivatives on different cancer cells have been extensively studied and these studies have led to the discovery of clinical candidates such as Phortress (Fig. 2) [25-30].

Prompted by the afore-mentioned findings and in the continuation of our ongoing research on oxadiazoles related to their anticancer activity [31], herein we described the design, synthesis of a new series of thiazole/benzothiazole-based oxadiazole derivatives (Fig. 3) and investigated their cytotoxic activity against A549 human lung adenocarcinoma, C6 rat glioma and NIH/3T3 mouse embryonic fibroblast cell lines. The most effective compounds were evaluated for their effects on apoptosis, caspase-3 activation, Akt, FAK, mitochondrial membrane potential and morphological changes in TEM micrographs. The most potent Akt and FAK inhibitor in this series was also analyzed for molecular docking interactions in the active sites of Akt (PDB code: 3OW4) and FAK (PDB code: 5TO8), respectively. Furthermore, a computational study was carried out to determine the physicochemical parameters of all compounds for the evaluation of their compliance to Lipinski's rule of five.

2. Results and Discussion

The synthesis of oxadiazole derivatives (**1-9**) followed the general pathway outlined in Scheme 1. Initially, 2-[(5,6,7,8-tetrahydronaphthalen-2-yl)oxy]acetic acid (**A**) was synthesized *via* the reaction of 5,6,7,8-tetrahydronaphthalen-2-ol with chloroacetic acid in the presence of sodium hydroxide. The treatment of compound **A** with ethanol afforded ethyl 2-[(5,6,7,8-tetrahydronaphthalen-2-yl)oxy]acetate (**B**). The reaction of the ester with hydrazine hydrate gave 2-[(5,6,7,8-tetrahydronaphthalen-2-yl)oxy]acetohydrazide (**C**). 5-[[[(5,6,7,8-Tetrahydronaphthalen-2-yl)oxy]methyl]-1,3,4-oxadiazole-2(3*H*)-thione (**D**) was obtained *via*

the ring closure reaction of compound **C** with carbon disulfide in the presence of potassium hydroxide. On the other hand, 2-chloro-*N*-(thiazol/benzothiazol-2-yl)acetamide derivatives were synthesized *via* the reaction of 2-aminothiazoles/2-aminobenzothiazoles with chloroacetyl chloride in the presence of triethylamine (TEA). In the last step, the nucleophilic substitution reaction of compound **D** with 2-chloro-*N*-(thiazol/benzothiazol-2-yl)acetamides in the presence of potassium carbonate afforded the target compounds (**1-9**). IR, ¹H NMR, ¹³C NMR, and mass spectral data were in agreement with the proposed structures of compounds **1-9**.

In the research for new anticancer agents, the most common screening methods are the screening tests against a panel of different cancer cell lines. In this study, MTT assay was carried out to determine the cytotoxic effects of the compounds on A549 human lung adenocarcinoma and C6 rat glioma cell lines (Table 1). Compounds **1**, **2**, **4**, **5**, **6**, **7** and **9** exhibited more significant cytotoxic activity against C6 cells than A549 cells, whereas compounds **3** and **8** were more effective on A549 cells than C6 cells.

Compound **6** was found to be the most promising anticancer agent in this series due to its significant inhibitory effects on C6 and A549 cell lines with IC₅₀ values of 4.63±0.85 μM and 39.33±4.04 μM, respectively. This compound was also more effective than cisplatin on both cell lines. This outcome indicated that the methoxy substituent at the 6th position of the benzothiazole ring significantly enhanced anticancer activity against both cell lines.

Compounds **9** and **2** exhibited notable cytotoxic activity against C6 cell line with IC₅₀ values of 66.67±12.58 and 89.33±14.47 μM, respectively. On the other hand, compounds **2** and **9** also showed anticancer activity against A549 cell line with IC₅₀ values of 91.67±7.64 and 115±5 μM, respectively.

MTT assay revealed that the chloro substituent at the 6th position of the benzothiazole ring decreased anticancer activity, whereas other substituents increased anticancer activity against C6 cell line. The ethoxy substituent at the 6th position of the benzothiazole ring decreased anticancer activity, whilst other substituents increased anticancer activity against A549 cell line.

Considering the anticancer effects of thiazole-substituted compounds **8** and **9** on A549 and C6 cell lines, it can be concluded that the nitro substituent at the 5th position of the thiazole ring increased anticancer activity against both cancer cells.

Toxicity to host cells is an important characteristic to assess the safety of drug candidates early in the drug discovery process. In order to evaluate whether the compounds were toxic or non-toxic to healthy cells, the viability of NIH/3T3 mouse embryonic fibroblast cells exposed to each compound was assessed using MTT assay (Table 1). The selectivity index (SI) values of the compounds were also determined to compare the selectivity of the compounds (Table 2). Compounds **2**, **6** and **9** were chosen for further studies due to their notable and selective antitumor effects on both cancer cells.

After 24 h incubation period, the apoptotic effects of compounds **2**, **6** and **9** were analyzed for A549 and C6 cells based on Annexin V-PI binding capacities in flow cytometry (Figs. 4 and 5). Following flow cytometric analyses, the early and late apoptotic effects of compounds **2**, **6** and **9** (for IC₅₀ doses) on C6 cell line were determined as 11.9%, 5.0% and 12.3%, while their viabilities were determined as 84.9%, 92.3%, 80.8%, respectively (Table 3, Fig. 4). On the other hand, the early and late apoptotic effects of compounds **2**, **6** and **9** (for IC₅₀ doses) on A549 cell line were determined as 17.0%, 12.2% and 25.3%, whereas their viabilities were determined as 79.1%, 71.7%, and 67.8%, respectively (Table 3, Fig. 5). According to these findings, compounds **2** and **9** (11.9 and 12.3%) showed similar apoptotic effects on C6 cells compared to cisplatin (11.4%). Compound **9** was also the most effective apoptotic compound (25.3%) on A549 cells compared to cisplatin (17.8%).

In order to investigate the effects of compounds **2**, **6** and **9** on mitochondrial membrane potential (MMP) of A549 and C6 cells, the cells were incubated by IC₅₀ concentrations of these compounds for 24 hours (Figs. 6 and 7, Table 4).

Compounds **2**, **6** and **9** caused higher disturbance on mitochondrial membrane potential in C6 cells than A549 cells. Mitochondrial membrane polarized C6 cell percentages of compounds **2**, **6**, **9** and cisplatin (for IC₅₀ doses) were determined as 32.6, 24.4, 0.6 and 45.1, while mitochondrial membrane depolarized C6 cell percentages of compounds **2**, **6**, **9** and cisplatin (for IC₅₀ doses) were determined as 60.1, 74.4, 98.0 and 55.0, respectively (Fig. 6 and Table 4). On the other hand, mitochondrial membrane polarized A549 cell percentages of compounds **2**, **6**, **9** and cisplatin (for IC₅₀ doses) were determined as 78.2, 69.8, 2.4 and 90.0, whilst mitochondrial membrane depolarized A549 cell percentages of compounds **2**, **6**, **9** and cisplatin (for IC₅₀ doses) were determined as 21.0, 27.9, 95.5 and 10.0, respectively (Fig. 7 and Table 4). According to these findings, compounds **2**, **6** and **9** were more effective than cisplatin on the depolarization of mitochondrial membrane in A549 and C6 cells.

Due to the key role of caspase-3 activation in the initiation of cellular events during early apoptotic process [32,33], the effects of compounds **2**, **6** and **9** on caspase-3 activation were determined. Caspase-3 positive cell percentages of compounds **2**, **6**, **9** and cisplatin (for IC₅₀ doses) were determined as 11.7, 33.9, 11.3 and 9.6, whereas caspase-3 negative cell percentages of compounds **2**, **6**, **9** and cisplatin (for IC₅₀ doses) were determined as 90.8, 69.8, 90.1 and 91.6 respectively, on C6 cell line (Fig. 8 and Table 5). On the other hand, caspase-3 (+) cell percentages of compounds **2**, **6**, **9** and cisplatin (for IC₅₀ doses) were determined as 7.1, 25.0, 5.4 and 10.5, whilst caspase-3 (-) cell percentages of compounds **2**, **6**, **9** and cisplatin (for IC₅₀ doses) were determined as 93.5, 76.4, 95.1, and 90.4, respectively, on A549 cell line (Fig. 9 and Table 5). These findings indicated that compound **6** was the most effective agent on caspase-3 activation in both cell lines.

As a consequence of the central role of Akt signaling in cancer [7-11], compounds **2**, **6** and **9** were investigated for their inhibitory effects on Akt activity (Table 6). Compound **6** inhibited Akt activity with an IC₅₀ value of 2.60±0.17 µM in C6 cell line more than cisplatin (IC₅₀= 39.00±1.41 µM) and GSK690693 (IC₅₀= 6.97±0.06 µM). Compound **6** also showed significant Akt inhibitory activity with an IC₅₀ value of 27.50±0.71 µM in A549 cell line when compared with cisplatin (IC₅₀= 34.00±1.73 µM) and GSK690693 (IC₅₀= 17.33±2.87 µM). On the other hand, compound **9** inhibited Akt kinase activity (IC₅₀= 44.50±3.53 µM) in C6 cell line similar to cisplatin. On the other hand, the significance of 1,3,4-oxadiazoles as FAK inhibitors [17-20] prompted us to evaluate the inhibitory effects of compounds **2**, **6**, **9** on FAK (Phospho-Tyr397) activity (Table 7). According to the assay, compound **6** showed significant FAK (Phospho-Tyr397) inhibitory activity with an IC₅₀ value of 19.50±2.12 µM in C6 cell line when compared with cisplatin (IC₅₀= 59.00±1.41 µM). However, compounds **2** and **9** did not cause significant FAK inhibition on C6 cells. This outcome pointed out the importance of the methoxy substituent at the 6th position of the benzothiazole ring for Akt and FAK inhibitory activities.

Molecular docking studies were performed to rationalize the observations of the biological activity of compound **6** to elucidate the possible binding modes of this compound in the active site of Akt when compared with GSK690693, a potent pan-AKT kinase inhibitor (PDB code: 3OW4) [34]. The docking results of compound **6** suggested that π-π interactions and hydrogen bonds were responsible for the observed affinity in the active site of Akt (Fig. 10). 6-Methoxybenzothiazole moiety of compound **6** presented π-π interactions with Arg4, Phe442 residues and H-bond with Asp439 residue. As compound **6** notably inhibited FAK, it

was also docked to the active site of FAK (PDB code: 5TO8) [35]. Molecular docking results indicated that 6-methoxybenzothiazole moiety of compound **6** formed π - π stacking with Phe568 residue and its acetamido group and oxadiazole moiety presented salt-bridge formation and π -cation with Lys457 residue in the active site of FAK (Fig. 11). The docking results of compound **6** in the active site of Akt and FAK pointed out that the presence of 6-methoxybenzothiazole moiety of this compound enhanced its inhibitory effects on these enzymes. Due to its high potency as a caspase-3 activator in this series, compound **6** was also analyzed for molecular docking interactions in the active site of caspase-3 (PDB codes: 4EHA and 4QTX) [36, 37]. Docking results of compound **6** in the active site of caspase-3 also indicated that compound **6** showed good binding affinity. 6-Methoxybenzothiazole, oxadiazole and tetrahydronaphthalene moieties of compound **6** presented π - π stacking and H-bonds with Arg207, Thr62 and Phe256 residues, respectively. However, the acetamido group of compound **6** was engaged in salt-bridge formation and H-bond with Arg207 in the active site of caspase-3 (Fig. 12). The docking score, glide gscore and glide emodel results of compound **6** were also given in Table 8.

The apoptosis results were consistent with TEM micrographs. At IC_{50} concentrations of compounds **2**, **6** and **9**, the shape of the treated cells became rounded, the cellular organization was disrupted, cell shrinkage, DNA condensation were observed and the membranes of organelles were sharply damaged indicating morphological changes of apoptosis in both cell lines (Figs. 13 and 14). The large vacuoles in the cytoplasm containing degraded cellular material also increased and the membranes were slightly damaged and nucleus fragmentation in A549 cell line incubated with compound **6** was shown (Fig. 13c). Furthermore, compound **6** significantly induced apoptotic morphological alterations causing chromatin condensation, large vacuoles and sharply damaged membranes in C6 cell line (Fig. 14c).

As a part of this study, Molinspiration software was used to determine their physicochemical parameters (log P, TPSA, nrotb, molecular weight, number of hydrogen bond donors and acceptors, molecular volume) for the evaluation of the compliance of the compounds to Lipinski's rule of five [38]. This rule states that most "drug like" molecules have $\log P \leq 5$, molecular weight ≤ 500 , number of hydrogen bond acceptors ≤ 10 , and number of hydrogen bond donors ≤ 5 . Compounds violating more than one of these rules may have bioavailability problems [38-41]. According to *in silico* studies, compound **3** only violated one parameter of Lipinski's rule of five, whereas other compounds did not violate

Lipinski's rule (Table 9). On the basis of Lipinski's rule of five, they were expected to have good oral bioavailability.

3. Conclusion

In conclusion, new thiazole/benzothiazole-based 1,3,4-oxadiazole derivatives were synthesized and evaluated for their cytotoxic effects on A549, C6 and NIH/3T3 cell lines. Compounds **2**, **6** and **9** were evaluated for their effects on apoptosis, caspase-3 activation, Akt, FAK, MMP and ultrastructural morphological changes.

In general, the compounds displayed more potent inhibitory effects on C6 cells than A549 cells. Compounds **2**, **6** and **9** were the most effective anticancer agents on A549 and C6 cell lines. In particular, compound **6** was identified as the most promising anticancer agent due to its significant antitumor effects on both cancer cell lines. Compound **6** increased caspase-3 cell population more than cisplatin on A549 and C6 cell lines. Compound **6** also showed significant Akt and FAK inhibitory activities. Docking studies confirmed that compound **6** showed high affinity to the active site of Akt comparing with GSK690693. This compound was able to form π - π interactions and hydrogen bond with proper residues. Docking results also confirmed that compound **6** formed reasonable interactions with Lys457 and Phe568 residues in the active site of FAK. Overall, the docking results were fundamentally in agreement with the biological data. Although all compounds caused apoptotic morphological alterations, compound **6** caused more significant morphological changes than other compounds on both cell lines. According to the *in vitro* and *in silico* studies, compound **6** stands out as a promising orally bioavailable anticancer drug candidate for further *in vivo* studies.

4. Experimental

4.1. Chemistry

All reagents were purchased from commercial suppliers and were used without further purification. The melting points (M.p.) of the compounds were determined on an Electrothermal 9100 melting point apparatus (Weiss-Gallenkamp, Loughborough, UK) and are uncorrected. IR spectra were recorded on an IRPrestige-21 Fourier Transform Infrared spectrophotometer (Shimadzu, Tokyo, Japan). ^1H NMR spectra were recorded on a Bruker spectrometer (Bruker, Billerica, MA, USA), whereas ^{13}C NMR spectra were recorded on a Varian Mercury-400 FT-NMR spectrometer (Agilent, Palo Alto, CA, USA). Mass spectra were recorded on a Shimadzu LCMS-IT-TOF system (Shimadzu, Kyoto, Japan). Thin Layer

Chromatography (TLC) was performed on TLC Silica gel 60 F₂₅₄ aluminium sheets (Merck, Darmstadt, Germany) to check the purity of the compounds.

4.1.1. General procedure for the synthesis of the compounds

4.1.1.1. 2-[(5,6,7,8-Tetrahydronaphthalen-2-yl)oxy]acetic acid (**A**)

Sodium 2-[(5,6,7,8-tetrahydronaphthalen-2-yl)oxy]acetate was obtained *via* the reaction of 5,6,7,8-tetrahydro-2-naphthol (0.05 mol) with chloroacetic acid (0.05 mol) in NaOH solution (0.12 mol in 25 mL water) under reflux for 6 h. Then the salt solution was acidified with sulphuric acid until compound **A** was precipitated. The solid was filtered off, washed with water and dried. The product was crystallized from ethanol [42].

4.1.1.2. Ethyl 2-[(5,6,7,8-tetrahydronaphthalen-2-yl)oxy]acetate (**B**)

A solution of (5,6,7,8-tetrahydronaphthalen-2-yl)oxyacetic acid (**A**) (0.04 mol) in ethanol (70 mL) in the presence of concentrated sulfuric acid (1 mL) was refluxed for 6 h. The obtained ester was poured into distilled water. The ester layer was extracted with ether. Then, the ether layer was washed with sodium bicarbonate solution and water. Ether layer was extracted again and dried with anhydrous sodium sulphate. Finally, organic ether phase was evaporated to obtain the product [42].

4.1.1.3. 2-[(5,6,7,8-Tetrahydronaphthalen-2-yl)oxy]acetohydrazide (**C**)

A mixture of ethyl 2-[(5,6,7,8-tetrahydronaphthalen-2-yl)oxy]acetate (**B**) (0.03 mol) and hydrazine hydrate (0.06 mol) in ethanol (50 mL) was refluxed for 2 h and the resulting solid product was filtered and dried. The product was crystallized from ethanol [42].

4.1.1.4. 5-[[[(5,6,7,8-Tetrahydronaphthalen-2-yl)oxy]methyl]-1,3,4-oxadiazole-2(3H)-thione (**D**)

A mixture of [(5,6,7,8-tetrahydronaphthalen-2-yl)oxy]acetohydrazide (**C**) (0.025 mol) and carbon disulfide (0.03 mol) in the presence of potassium hydroxide (0.025 mol) in ethanol (50 mL) was refluxed for 6 h. The solution was cooled and acidified with hydrochloric acid solution. The solid was filtered off, washed with water and dried. The product was crystallized from ethanol.

4.1.1.5. 2-Chloro-N-(aryl)acetamides

Chloroacetyl chloride (0.03 mol) was added dropwise with stirring to a mixture of aromatic amine (0.025 mol) and TEA (0.025 mol) in toluene (50 mL) at 0-5 °C. The solvent

was evaporated under reduced pressure. The residue was washed with water to remove TEA and crystallized from ethanol. The products were crystallized from ethanol [43].

4.1.1.6. *N*-(Aryl)-2-[[5-[[5,6,7,8-tetrahydronaphthalen-2-yl)oxy)methyl]-1,3,4-oxadiazol-2-yl]thio]acetamide (**1-9**)

A mixture of 5-[[5,6,7,8-tetrahydronaphthalen-2-yl)oxy)methyl]-1,3,4-oxadiazole-2(3*H*)-thione (**D**) (0.0015 mol) and appropriate 2-chloro-*N*-(aryl)acetamide (0.0015 mol) in acetone (25 mL) was stirred at room temperature for 8 h in the presence of potassium carbonate (0.0015 mol). The solvent was evaporated under reduced pressure. The residue was washed with water and crystallized from ethanol.

4.1.1.6.1. *N*-(Benzothiazol-2-yl)-2-[[5-[[5,6,7,8-tetrahydronaphthalen-2-yl)oxy)methyl]-1,3,4-oxadiazol-2-yl]thio]acetamide (**1**)

Yield: 85%. M.p. 214-215 °C.

IR ν_{\max} (cm⁻¹): 3174.83, 3138.18 (N-H stretching), 3061.03 (aromatic C-H stretching), 2964.59, 2929.87, 2860.43 (aliphatic C-H stretching), 1681.93 (amide C=O stretching), 1598.99, 1562.34, 1500.62, 1481.33 (N-H bending, C=N and C=C stretching), 1438.90, 1381.03 (C-H bending), 1325.10, 1259.52, 1232.51, 1165.00, 1122.57, 1028.06, 1012.63 (C-N, C-O stretching and aromatic C-H in plane bending), 987.55, 869.90, 823.60, 792.74, 758.02, 690.52, 671.23 (aromatic C-H out of plane bending and C-S stretching).

¹H NMR (500 MHz, DMSO-*d*₆) δ (ppm): 1.68 (s, 4H), 2.62 (d, *J* = 16 Hz, 4H), 4.47 (s, 2H), 5.30 (s, 2H), 6.71-6.75 (m, 2H), 6.93 (d, *J* = 8.5 Hz, 1H), 7.33 (t, *J* = 7.5 Hz, 1H), 7.46 (t, *J* = 7.5 Hz, 8.0 Hz, 1H), 7.78 (d, *J* = 8.0 Hz, 1H), 7.99 (d, *J* = 8.0 Hz, 1H), 12.79 (s, 1H).

¹³C NMR (100 MHz, DMSO-*d*₆) δ (ppm): 22.67 (d, *J* = 26.6 Hz, 2CH₂), 27.91 (CH₂), 28.95 (CH₂), 35.65 (CH₂), 59.40 (CH₂), 114.67 (2CH), 120.66 (CH), 121.74 (CH), 123.73 (CH), 126.20 (CH), 129.79 (CH), 129.94 (C), 131.44 (C), 137.82 (C), 148.41 (C), 154.95 (C), 157.64 (C), 164.01 (C), 164.06 (C), 166.21 (C).

HRMS (ESI) (*m/z*): [M+H]⁺ calcd. for C₂₂H₂₀N₄O₃S₂: 453.1050, found: 453.1040.

4.1.1.6.2. *N*-(6-Fluorobenzothiazol-2-yl)-2-[[5-[[5,6,7,8-tetrahydronaphthalen-2-yl)oxy)methyl]-1,3,4-oxadiazol-2-yl]thio]acetamide (**2**)

Yield: 81%. M.p. 219-220 °C.

IR ν_{\max} (cm^{-1}): 3188.33 (N-H stretching), 3091.89 (aromatic C-H stretching), 2931.80, 2879.72 (aliphatic C-H stretching), 1681.93 (amide C=O stretching), 1610.56, 1570.06, 1500.62, 1481.33, 1456.26 (N-H bending, C=N and C=C stretching), 1381.03 (C-H bending), 1336.67, 1259.52, 1246.02, 1197.79, 1163.08, 1120.64, 1055.06, 1037.70, 1002.98 (C-N, C-O stretching and aromatic C-H in plane bending), 977.91, 912.33, 891.11, 854.47, 794.67, 746.45, 692.44 (aromatic C-H out of plane bending and C-S stretching).

^1H NMR (500 MHz, DMSO- d_6) δ (ppm): 1.67-1.68 (m, 4H), 2.62 (d, J = 15.5 Hz, 4H), 4.47 (s, 2H), 5.30 (s, 2H), 6.70-6.75 (m, 2H), 6.93 (d, J = 8.5 Hz, 1H), 7.31 (td, J = 3.0 Hz, 2.5 Hz, 1H), 7.79 (dd, J = 9.0 Hz, J = 5.0 Hz, 1H), 7.91 (dd, J = 8.75 Hz, J = 3.0 Hz, 2.5 Hz, 1H), 12.82 (brs, 1H).

^{13}C NMR (100 MHz, DMSO- d_6) δ (ppm): 22.60 (d, J = 26.7 Hz, 2CH₂), 27.85 (CH₂), 28.89 (CH₂), 35.55 (CH₂), 59.42 (CH₂), 108.10 (d, J = 27.5 Hz, CH), 112.46 (CH), 114.24 (d, J = 24.3 Hz, CH), 114.67 (CH), 121.74 (d, J = 9.1 Hz, CH), 129.71 (CH), 129.93 (C), 132.67 (d, J = 11.4 Hz, C), 137.78 (C), 145.12 (C), 154.93 (C), 157.53 (d, J = 8.4 Hz, C), 159.88 (C), 163.94 (C), 163.98 (C), 166.24 (C).

HRMS (ESI) (m/z): $[\text{M}+\text{H}]^+$ calcd. for C₂₂H₁₉FN₄O₃S₂: 471.0955, found: 471.0940.

4.1.1.6.3. *N*-(6-Chlorobenzothiazol-2-yl)-2-[[5-[(5,6,7,8-tetrahydronaphthalen-2-yl)oxy)methyl]-1,3,4-oxadiazol-2-yl]thio]acetamide (**3**)

Yield: 88%. M.p. 208-209 °C.

IR ν_{\max} (cm^{-1}): 3174.83, 3138.18 (N-H stretching), 3080.32, 3055.24 (aromatic C-H stretching), 2929.87, 2858.51 (aliphatic C-H stretching), 1681.93 (amide C=O stretching), 1602.85, 1568.13, 1500.62, 1471.69 (N-H bending, C=N and C=C stretching), 1438.90, 1382.96 (C-H bending), 1336.67, 1263.37, 1232.51, 1170.79, 1122.57, 1097.50, 1056.99, 1035.77, 1002.98 (C-N, C-O stretching and aromatic C-H in plane bending), 987.55, 975.98, 866.04, 808.17, 761.88, 688.59 (aromatic C-H out of plane bending and C-S stretching).

^1H NMR (500 MHz, DMSO- d_6) δ (ppm): 1.68 (s, 4H), 2.62 (d, J = 10.5 Hz, 4H), 4.46 (s, 2H), 5.30 (s, 2H), 6.70-6.74 (m, 2H), 6.93 (d, J = 7.5 Hz, 1H), 7.48 (d, J = 7.0 Hz, 2H), 8.14 (s, 1H), 12.88 (s, 1H).

^{13}C NMR (100 MHz, DMSO- d_6) δ (ppm): 22.66 (d, J = 26.7 Hz, 2CH₂), 27.91 (CH₂), 28.94 (CH₂), 35.59 (CH₂), 59.39 (CH₂), 112.46 (CH), 114.65 (CH), 121.46 (CH), 121.87 (CH),

126.55 (CH), 127.81 (C), 129.77 (CH), 129.92 (C), 133.14 (C), 137.80 (C), 147.31 (C), 154.95 (C), 158.47 (C), 164.01 (2C), 166.42 (C).

HRMS (ESI) (m/z): $[M+H]^+$ calcd. for $C_{22}H_{19}ClN_4O_3S_2$: 487.0660, found: 487.0652.

4.1.1.6.4. *N*-(6-Nitrobenzothiazol-2-yl)-2-[[5-[(5,6,7,8-tetrahydronaphthalen-2-yl)oxy)methyl]-1,3,4-oxadiazol-2-yl]thio]acetamide (**4**)

Yield: 90%. M.p. 212-213 °C.

IR ν_{max} (cm^{-1}): 3172.90, 3138.18 (N-H stretching), 3080.32, 3049.46 (aromatic C-H stretching), 2926.01, 2858.51 (aliphatic C-H stretching), 1695.43 (amide C=O stretching), 1610.56, 1575.84, 1558.48, 1521.84, 1500.62, 1467.83 (N-H bending, NO_2 , C=N vs C=C stretching), 1446.61, 1381.03 (C-H bending), 1334.74, 1269.16, 1232.51, 1166.93, 1124.50, 1058.92, 1039.63 (C-N, C-O stretching and aromatic C-H in plane bending), 985.62, 902.69, 821.68, 786.96, 742.59, 719.45, 682.80 (aromatic C-H out of plane bending and C-S stretching).

1H NMR (500 MHz, DMSO- d_6) δ (ppm): 1.66 (s, 4H), 2.60 (d, $J=16.5$ Hz, 4H), 4.50 (s, 2H), 5.29 (s, 2H), 6.70-6.73 (m, 2H), 6.91 (d, $J=8.5$ Hz, 1H), 7.91 (d, $J=8.5$ Hz, 1H), 8.28 (d, $J=8.5$ Hz, 1H), 9.04 (s, 1H), 13.19 (s, 1H).

^{13}C NMR (100 MHz, DMSO- d_6) δ (ppm): 22.66 (d, $J=26.7$ Hz, $2CH_2$), 27.90 (CH_2), 28.95 (CH_2), 35.69 (CH_2), 59.39 (CH_2), 112.44 (CH), 114.62 (CH), 119.02 (CH), 120.74 (CH), 121.74 (CH), 129.76 (CH), 129.91 (C), 132.19 (C), 137.79 (C), 143.07 (C), 153.31 (C), 154.94 (C), 163.16 (C), 163.98 (C), 164.05 (C), 167.02 (C).

HRMS (ESI) (m/z): $[M+H]^+$ calcd. for $C_{22}H_{19}N_5O_5S_2$: 498.0900, found: 498.0883.

4.1.1.6.5. *N*-(6-Methylbenzothiazol-2-yl)-2-[[5-[(5,6,7,8-tetrahydronaphthalen-2-yl)oxy)methyl]-1,3,4-oxadiazol-2-yl]thio]acetamide (**5**)

Yield: 77%. M.p. 218-219 °C.

IR ν_{max} (cm^{-1}): 3184.48, 3155.54 (N-H stretching), 3072.60 (aromatic C-H stretching), 2972.31, 2933.73, 2860.43 (aliphatic C-H stretching), 1683.86 (amide C=O stretching), 1608.63, 1573.91, 1556.55, 1500.62, 1479.40, 1460.11 (N-H bending, C=N and C=C stretching), 1381.03 (C-H bending), 1330.88, 1261.45, 1230.58, 1165.00, 1120.64, 1056.99, 1033.85, 1004.91 (C-N, C-O stretching and aromatic C-H in plane bending), 989.48, 819.75, 792.74, 746.45, 690.52, 665.44 (aromatic C-H out of plane bending and C-S stretching).

^1H NMR (500 MHz, DMSO- d_6) δ (ppm): 1.68 (s, 4H), 2.42 (s, 3H), 2.63 (d, J = 14.5 Hz, 4H), 4.45 (s, 2H), 5.30 (s, 2H), 6.71-6.75 (m, 2H), 6.94 (d, J = 8.0 Hz, 1H), 7.27 (d, J = 7.5 Hz, 1H), 7.66 (d, J = 8.0 Hz, 1H), 7.77 (s, 1H), 12.70 (s, 1H).

^{13}C NMR (100 MHz, DMSO- d_6) δ (ppm): 20.86 (CH₃), 22.59 (d, J = 26.7 Hz, 2CH₂), 27.84 (CH₂), 28.88 (CH₂), 35.57 (CH₂), 59.42 (CH₂), 112.46 (CH), 114.69 (CH), 120.21 (CH), 121.21 (CH), 127.44 (CH), 129.70 (CH), 129.93 (C), 131.54 (C), 133.17 (C), 137.77 (C), 154.93 (2C), 157.64 (C), 163.95 (2C), 166.42 (C).

HRMS (ESI) (m/z): [M+H]⁺ calcd. for C₂₃H₂₂N₄O₃S₂: 467.1206, found: 467.1190.

4.1.1.6.6. *N*-(6-Methoxybenzothiazol-2-yl)-2-[[5-[(5,6,7,8-tetrahydronaphthalen-2-yl)oxy)methyl]-1,3,4-oxadiazol-2-yl]thio]acetamide (**6**)

Yield: 79%. M.p. 207-208 °C.

IR ν_{max} (cm⁻¹): 3192.19 (N-H stretching), 3089.96 (aromatic C-H stretching), 2927.94 (aliphatic C-H stretching), 1681.93 (amide C=O stretching), 1610.56, 1579.70, 1562.34, 1500.62, 1469.76 (N-H bending, C=N and C=C stretching), 1429.25, 1382.96 (C-H bending), 1338.60, 1257.59, 1224.80, 1170.79, 1122.57, 1056.99, 1028.06, 1002.98 (C-N, C-O stretching and aromatic C-H in plane bending), 821.68, 796.60, 748.38, 692.44 (aromatic C-H out of plane bending and C-S stretching).

^1H NMR (500 MHz, DMSO- d_6) δ (ppm): 1.68 (s, 4H), 2.62 (d, J = 15.5 Hz, 4H), 3.81 (s, 3H), 4.44 (s, 2H), 5.30 (s, 2H), 6.71-6.75 (m, 2H), 6.94 (d, J = 8.5 Hz, 1H), 7.04-7.06 (m, 1H), 7.57-7.58 (m, 1H), 7.67 (d, J = 8.5 Hz, 1H), 12.65 (s, 1H).

^{13}C NMR (100 MHz, DMSO- d_6) δ (ppm): 22.63 (d, J = 26.0 Hz, 2CH₂), 27.88 (CH₂), 28.92 (CH₂), 35.56 (CH₂), 55.59 (CH₃), 59.41 (CH₂), 104.71 (CH), 112.48 (CH), 114.68 (CH), 114.99 (CH), 121.24 (CH), 129.75 (CH), 129.94 (C), 132.76 (C), 137.80 (C), 142.48 (C), 154.94 (C), 155.51 (C), 156.25 (C), 163.97 (C), 164.01 (C), 165.82 (C).

HRMS (ESI) (m/z): [M+H]⁺ calcd. for C₂₃H₂₂N₄O₄S₂: 483.1155, found: 483.1139.

4.1.1.6.7. *N*-(6-Ethoxybenzothiazol-2-yl)-2-[[5-[(5,6,7,8-tetrahydronaphthalen-2-yl)oxy)methyl]-1,3,4-oxadiazol-2-yl]thio]acetamide (**7**)

Yield: 78%. M.p. 216-217 °C.

IR ν_{max} (cm⁻¹): 3196.05 (N-H stretching), 3088.03 (aromatic C-H stretching), 2983.88, 2929.87, 2881.65 (aliphatic C-H stretching), 1685.79 (amide C=O stretching), 1610.56,

1560.41, 1502.55, 1479.40, 1458.18 (N-H bending, C=N and C=C stretching), 1386.82 (C-H bending), 1342.46, 1263.37, 1249.87, 1228.66, 1161.15, 1111.00, 1060.85, 1029.99 (C-N, C-O stretching and aromatic C-H in plane bending), 999.13, 941.26, 891.11, 850.61, 808.17, 748.38, 694.37, 665.44 (aromatic C-H out of plane bending and C-S stretching).

^1H NMR (500 MHz, DMSO- d_6) δ (ppm): 1.11 (t, J = 7.0 Hz, 3H), 1.43 (s, 4H), 2.38 (d, J = 15.5 Hz, 4H), 3.82 (q, J = 7.0 Hz, 2H), 4.18 (s, 2H), 5.05 (s, 2H), 6.47-6.50 (m, 2H), 6.69 (d, J = 8.0 Hz, 1H), 6.77-6.79 (m, 1H), 7.29-7.30 (m, 1H), 7.40 (d, J = 8.5 Hz, 1H), 12.38 (brs, 1H).

^{13}C NMR (100 MHz, DMSO- d_6) δ (ppm): 14.59 (CH₃), 22.61 (d, J = 26.6 Hz, 2CH₂), 27.86 (CH₂), 28.89 (CH₂), 35.65 (CH₂), 59.42 (CH₂), 63.58 (CH₂), 105.00 (CH), 112.48 (CH), 114.69 (CH), 115.28 (CH), 121.16 (CH), 129.72 (CH), 129.93 (C), 132.76 (C), 137.79 (C), 142.44 (C), 154.94 (C), 155.40 (C), 155.73 (C), 163.93 (C), 164.01 (C), 165.89 (C).

HRMS (ESI) (m/z): [M+H]⁺ calcd. for C₂₄H₂₄N₄O₄S₂: 497.1312, found: 497.1299.

4.1.1.6.8. *N*-(Thiazol-2-yl)-2-[[5-[(5,6,7,8-tetrahydronaphthalen-2-yl)oxy)methyl]-1,3,4-oxadiazol-2-yl]thio]acetamide (**8**)

Yield: 83%. M.p. 204-205 °C.

IR ν_{max} (cm⁻¹): 3199.91 (N-H stretching), 3072.60 (aromatic C-H stretching), 2931.80, 2850.79, 2752.42 (aliphatic C-H stretching), 1691.57 (amide C=O stretching), 1591.27, 1502.55, 1463.97 (N-H bending, C=N and C=C stretching), 1436.97, 1382.96 (C-H bending), 1332.81, 1309.67, 1267.23, 1246.02, 1232.51, 1170.79, 1161.15, 1107.14, 1049.28, 1029.99 (C-N, C-O stretching and aromatic C-H in plane bending), 972.12, 929.69, 823.60, 813.96, 800.46, 775.38, 729.09, 694.37, 623.01 (aromatic C-H out of plane bending and C-S stretching).

^1H NMR (500 MHz, DMSO- d_6) δ (ppm): 1.69 (s, 4H), 2.65 (d, J = 21.0 Hz, 4H), 4.40 (s, 2H), 5.30 (s, 2H), 6.73-6.76 (m, 2H), 6.96 (d, J = 8.5 Hz, 1H), 7.26 (d, J = 3.5 Hz, 1H), 7.51 (d, J = 3.5 Hz, 1H), 12.53 (s, 1H).

^{13}C NMR (100 MHz, DMSO- d_6) δ (ppm): 23.16 (d, J = 26.7 Hz, 2CH₂), 28.41 (CH₂), 29.45 (CH₂), 35.85 (CH₂), 59.92 (CH₂), 113.03 (CH), 114.34 (CH), 115.21 (CH), 130.28 (CH), 130.47 (C), 137.79 (CH), 138.32 (C), 155.45 (C), 158.18 (C), 164.45 (C), 164.55 (C), 165.53 (C).

HRMS (ESI) (m/z): [M+H]⁺ calcd. for C₁₈H₁₈N₄O₃S₂: 403.0893, found: 403.0887.

4.1.1.6.9. *N*-(5-Nitrothiazol-2-yl)-2-[[5-[(5,6,7,8-tetrahydronaphthalen-2-yl)oxy)methyl]-1,3,4-oxadiazol-2-yl]thio]acetamide (**9**)

Yield: 82%. M.p. 181-182 °C.

IR ν_{\max} (cm⁻¹): 3157.47 (N-H stretching), 2929.87, 2854.65 (aliphatic C-H stretching), 1691.57 (amide C=O stretching), 1593.20, 1573.91, 1519.91, 1475.54 (N-H bending, NO₂, C=N and C=C stretching), 1421.54, 1346.31 (C-H bending), 1301.95, 1255.66, 1168.86, 1122.57, 1055.06, 1037.70 (C-N, C-O stretching and aromatic C-H in plane bending), 966.34, 902.69, 864.11, 823.60, 802.39, 731.02, 694.37 (aromatic C-H out of plane bending and C-S stretching).

¹H NMR (500 MHz, DMSO-*d*₆) δ (ppm): 1.69 (t, *J* = 3 Hz, 4H), 2.64 (d, *J* = 21.5 Hz, 4H), 4.39 (s, 2H), 5.30 (s, 2H), 6.72-6.76 (m, 2H), 6.95 (d, *J* = 8.5 Hz, 1H), 8.58 (s, 1H), 13.19 (s, 1H).

¹³C NMR (100 MHz, DMSO-*d*₆) δ (ppm): 22.69 (d, *J* = 26.7 Hz, 2CH₂), 27.94 (CH₂), 28.98 (CH₂), 36.72 (CH₂), 59.45 (CH₂), 112.54 (CH), 114.71 (CH), 129.80 (CH), 129.99 (C), 137.85 (C), 140.27 (C), 143.59 (CH), 154.99 (C), 163.90 (C), 164.30 (C), 165.39 (C), 169.26 (C).

HRMS (ESI) (*m/z*): [M+H]⁺ calcd. for C₁₈H₁₇N₅O₅S₂: 448.0744, found: 448.0738.

4.2. Biochemistry

4.2.1. Cell culture and drug treatment

The cell lines used in this work were obtained from American Type Culture Collection (ATCC). C6 Rat glioma, A549 human lung adenocarcinoma, and NIH/3T3 mouse embryonic fibroblast cells were cultured and drug treatments were carried out as previously described [44].

4.2.2. MTT assay

The level of cellular 3-(4,5-dimethylthiazol-2-yl)-2,5-diphenyltetrazolium bromide (MTT) (Sigma-Aldrich, St. Louis, MO, USA) reduction was quantified as previously described in the literature [44] with small modifications [45]. Cisplatin and GSK690693 were used as positive controls. Selectivity index (SI) values were also calculated according to the formula [46] below:

$$SI = IC_{50} \text{ for normal cell line} / IC_{50} \text{ for cancerous cell line}$$

4.2.3. Flow cytometric analyses of apoptosis

After the incubation of A549 and C6 cells with compounds **2**, **6**, **9** and cisplatin at IC_{50} concentrations, phosphatidylserine externalization, which indicates early apoptosis, was measured by FITC Annexin V apoptosis detection kit (BD Pharmingen, San Jose, CA, USA) on a BD FACS Aria flow cytometer for 24 h. Annexin V staining protocol was applied according to the manufacturer's instructions (BD Pharmingen, San Jose, CA, USA). The data were analyzed by a BD FACS Aria flow cytometer using FACSDiva version 6.1.1 software.

4.2.4. Analysis of mitochondrial membrane potential (JC1) by flow cytometry

The cells were seeded in six-well plates at a density of 10^5 cells/mL, and the IC_{50} doses of compounds **2**, **6**, **9** and cisplatin were added to cells. The cells were incubated in 5% CO_2 air-conditioned atmosphere at 37 °C. After 24 h of incubation, mitochondrial membrane potential protocol was applied according to the manufacturer's instructions (BD Pharmingen, San Jose, CA, USA) and analyzed by a BD FACS Aria flow cytometer using FACSDiva version 6.1.1 software.

4.2.5. Flow cytometric analyses of caspase-3

After A549 and C6 cells were incubated with compounds **2**, **6**, **9** and cisplatin at IC_{50} concentrations for 24 h, caspase-3 activity measurement protocol was applied according to manufacturer's instructions (BD Pharmingen, San Jose, CA, USA). In brief, the cells were washed with cold phosphate buffer solution (PBS) 1X cells and incubated with 0.5 mL perm lyse solution for 30 min at room temperature in the dark. Pellets were washed twice with 0.5 mL perm wash buffer. Cells were resuspended in 100 μ L perm wash buffer, and 10 μ L caspase-3 antibody was added for 20 min at room temperature in the dark. At least 10,000 cells were counted for each sample and cells were analyzed by flow cytometry using FACSDiva version 6.1.1 software.

4.2.6. Inhibition of Akt enzyme

After 10,000 cells/well were incubated with compounds **2**, **6**, **9** and cisplatin at IC_{50} concentrations for 24 h, in cell ELISA colorimetric Akt activity protocol was applied according to the manufacturer's instructions (Thermo Fisher Scientific, Waltham, MA, USA). Briefly, the media was removed and 100 μ L of 4% formaldehyde was added to each well. The plate was incubated in a fume hood at room temperature for 15 minutes. Formaldehyde was removed and plate was washed twice with 100 μ L/well of 1X TBS. 1X TBS was removed, 100 μ L/well of 1X permeabilization buffer was added and incubated for 15 minutes at room temperature. Permeabilization buffer was removed and plate was washed once with 100

$\mu\text{L}/\text{well}$ of 1X TBS. 1X TBS was removed, 100 $\mu\text{L}/\text{well}$ quenching solution was added and incubated at room temperature for 20 minutes. Quenching Solution was removed and plate was washed once with 100 $\mu\text{L}/\text{well}$ of 1X TBS. Then, 1X TBS was removed and 100 $\mu\text{L}/\text{well}$ of blocking buffer was added and incubated at room temperature for 30 minutes. After blocking buffer was removed, 50 $\mu\text{L}/\text{well}$ of primary antibody was added. A plate sealer was applied and incubated overnight at 4 °C. The primary antibody solution was removed and plate was washed three times with 100 $\mu\text{L}/\text{well}$ of 1X wash buffer. After wash buffer was removed, 100 $\mu\text{L}/\text{well}$ of diluted HRP conjugate was added and incubated for 30 minutes at room temperature. Wash buffer was removed and 100 $\mu\text{L}/\text{well}$ of TMB substrate was added. Then plate was incubated at room temperature, protected from light. 100 $\mu\text{L}/\text{well}$ of TMB stop solution was added and the absorbance was measured at 450 nm within 30 minutes of stopping the reaction. The experiment was performed in triplicate wells. The values of blank wells were subtracted from each well of treated and control cells. Percent Akt activity was defined as the relative absorbance of treated versus untreated control cells. IC_{50} values were determined from graphics using three different concentrations.

4.2.7. FAK (Phospho-Tyr397) Activity Detection by ELISA

The effects of compounds **2**, **6**, **9** and cisplatin on FAK (Phospho-Tyr397) activity were determined by Colorimetric Cell-Based ELISA FAK (Phospho-Tyr397) activity kit (Aviva Systems Biology, San Diego, USA). C6 cells were administrated by IC_{50} concentrations of compound **2**, **6**, **9** and cisplatin for 24 hours. Cells were rinsed with 200 μL of 1 x TBS twice. Cells were fixed by incubating with 100 μL of fixing solution for 20 minutes at room temperature by 4% formaldehyde. Fixing solution was removed and the plate was washed 3 times with 200 μL 1 x wash buffer for five minutes each time with gentle shaking on the orbital shaker. Then, 100 μL quenching buffer was added and incubated for 20 minutes at room temperature. Plate was washed 3 times with 1 x wash buffer for 5 minutes at a time. Then, 200 μL of blocking buffer was added and incubated for 1 hour at room temperature and washed 3 times with 200 μL of 1 x wash buffer for 5 minutes at a time. 50 μL of 1 x primary antibodies (Anti-FAK (Phospho-Tyr397) antibody, Anti-FAK antibody and/or Anti-GAPDH antibody) was added to the corresponding wells, covered with parafilm and incubated for 16 hours (overnight) at 4 °C. Then plate was washed 3 times with 200 μL of 1x wash buffer for 5 minutes at a time. 50 μL of 1 x secondary antibodies (HRP-Conjugated anti-rabbit IgG and/or HRP-conjugated anti-mouse IgG) was added to corresponding wells and incubated for 1.5 hours at room temperature with gentle shaking on the shaker. Plate was

washed 3 times with 200 μ L of 1x wash buffer for 5 minutes at a time, and 50 μ L of ready-to-use substrate was added to each well and incubated for 30 minutes at room temperature in the dark with gentle shaking on the shaker. 50 μ L of stop solution was added to each well and read OD at 450 nm immediately using an ELx808-IU BioTek apparatus. Every concentration was repeated in double wells. The OD₄₅₀ values obtained for the phosphorylated FAK was normalized using the OD₄₅₀ values obtained for GAPDH. IC₅₀ values were determined from graphics using three different concentrations.

4.2.8. Transmission Electron Microscopy (TEM)

TEM (TEM FEI Tecnai BioTWIN; Hillsboro, OR, USA) was processed for ultrastructural changes. C6 and A549 cells grown in DMEM and RPMI, respectively, were incubated with compounds **2**, **6**, **9** and cisplatin at IC₅₀ values for 24 h. They were then fixed with 2.5% glutaraldehyde in 0.1 M PBS at pH 7.4 and left in PBS overnight at 4 °C. After being embedded in agar and post fixation in 2% osmium tetroxide, cells were dehydrated in graded ethanol: 70, 90, 96 and 100%. Then cells were embedded in EPON 812 epoxy (Sigma Aldrich, Seelze, Germany) and sectioned on ultramicrotome (Leica EM UC6; Wetzlar, Germany).

4.2.9. Statistical analyses

Statistical Package for the Social Sciences (SPSS) for Windows 15.0 was used for statistical analysis. Data was expressed as Mean \pm SD. Comparisons were performed by one way ANOVA test for normally distributed continuous variables and post hoc analyses of group differences were expressed by the Tukey test.

4.2.10. Molecular docking studies

Compound **6** was docked to the active site of Akt together with GSK690693, FAK and caspase-3. Ligands were prepared with energy minimization in ligand preparation program of Schrödinger's Maestro molecular modeling package (Schrödinger Release 2016-2: Schrödinger, LLC, New York, NY, USA) at physiological pH (pH= 7.4) using Optimized Potential Liquid Simulations (OPLS_2005) force field and crystal structures of Akt, FAK and caspase-3 were retrieved from Protein Data Bank server (PDB codes: 3OW4 for Akt; 5TO8 for FAK; 4EHA and 4QTX for caspase-3) and optimized for docking analysis in protein preparation module of Schrödinger's Maestro molecular modeling package. In molecular docking simulations: Glide/XP docking protocols were applied for the prediction of topologies of compound **6** and GSK690693 in the active sites of target structures [34-37].

4.2.11. Molinspiration calculations

The physicochemical parameters (log P, TPSA, nrotb, molecular weight, number of hydrogen bond donors and acceptors, molecular volume) of compounds **1-9** were calculated using Molinspiration software [37-40].

Acknowledgements

This study was supported by Anadolu University Scientific Research Projects Commission under the grant no: 1402S054.

References

- [1] K. Nepali, S. Sharma, M. Sharma, P.M.S. Bedi, K.L. Dhar, *Eur. J. Med. Chem.* 77 (2014) 422–487.
- [2] S.H. Hassanpour, M. Dehghani, *J. Cancer Res. Pract.* 4 (2017) 127–129.
- [3] K. Papat, K. McQueen, T.W. Feeley, *Best Pract. Res. Clin. Anaesthesiol.* 27 (2013) 399–408.
- [4] S. Nussbaumer, P. Bonnabry, J.-L. Veuthey, S. Fleury-Souverain, *Talanta* 85 (2011) 2265–2289.
- [5] C. Holohan, S. Van Schaeuybroeck, D.B. Longley, P.G. Johnston, *Nat. Rev. Cancer* 13 (2013) 714–726.
- [6] J. Foo, F. Michor, *J. Theor. Biol.* 355 (2014) 10–20.
- [7] G.M. Nitulescu, D. Margina, P. Juzenas, Q. Peng, O.T. Olaru, E. Saloustros, C. Fenga, D.A. Spandidos, M. Libra, A.M. Tsatsakis, *Int. J. Oncol.* 48 (2016) 869–885.
- [8] J.K. Morrow, L. Du-Cuny, L. Chen, E.J. Meuillet, E.A. Mash, G. Powis, S. Zhang, *Recent Pat. Anti-Cancer Drug Discov.* 6 (2011) 146–159.
- [9] K.A. McDowell, G.J. Riggins, G.L. Gallia, *Curr. Pharm. Des.* 17 (2011) 2411–2420.
- [10] G. Cassinelli, V. Zuco, L. Gatti, C. Lanzi, N. Zaffaroni, D. Colombo, P. Perego, *Curr. Med. Chem.* 20 (2013) 1923–1945.
- [11] J.S. Brown, U. Banerji, *Pharmacol. Ther.* 172 (2017) 101–115.
- [12] B.Y. Lee, P. Timpson, L.G. Horvath, R.J. Daly, *Pharmacol. Ther.* 146 (2015) 132–149.
- [13] M. Roy-Luzarraga, K. Hodivala-Dilke, *Clin. Cancer Res.* 22 (2016) 3718–3724.

- [14] H. Yoon, J.P. Dehart, J.M. Murphy, S.-T. Steve Lim, J. Histochem. Cytochem. 63 (2015) 114–128.
- [15] X. Zhao, J.-L. Guan, Adv. Drug Deliv. Rev. 63 (2011) 610–615.
- [16] F.-Y. Cao, X.-P. Zhou, J. Sub, X.-H. Yang, F.-H. Mu, J.-Y. Shen, W. Sun, Anti-Cancer Agents Med. Chem. 16 (2016) 934–941.
- [17] J. Boström, A. Hogner, A. Llinàs, E. Wellner, A.T. Plowright, J. Med. Chem. 55 (2012) 1817–1830.
- [18] A. Zarghi, Z. Hajimahdi, Expert Opin. Ther. Patents 23 (2013) 1209–1232.
- [19] I. Khan, A. Ibrar, N. Abbas, Arch. Pharm. Chem. Life Sci. 347 (2014) 1–20.
- [20] S. Bajaj, V. Asati, J. Singh, P.P. Roy, Eur. J. Med. Chem. 97 (2015) 124–141.
- [21] A. Ayati, S. Emami, A. Asadipour, A. Shafiee, A. Foroumadi, Eur. J. Med. Chem. 97 (2015) 699–718.
- [22] D. Das, P. Sikdar, M. Bairagi, Eur. J. Med. Chem. 109 (2016) 89–98.
- [23] R. Morigi, A. Locatelli, A. Leoni, M. Rambaldi, Recent Pat. Anti-Cancer Drug Discov. 10 (2015) 280–297.
- [24] S. Jain, S. Pattnaik, K. Pathak, S. Kumar, D. Pathak, S. Jain, A. Vaidya, Mini Rev. Med. Chem. 18(8) (2018) 640–655.
- [25] A. Rouf, C. Tanyeli, Eur. J. Med. Chem. 97 (2015) 911–927.
- [26] M.N. Noolvi, H.M. Patel, M. Kaur, Eur. J. Med. Chem. 54 (2012) 447–462.
- [27] R.S. Keri, M.R. Patil, S.A. Patil, S. Budagumpi, Eur. J. Med. Chem. 89 (2015) 207–251.
- [28] P.C. Sharma, A. Sinhmar, A. Sharma, H. Rajak, D.P. Pathak, J. Enzyme Inhib. Med. Chem. 28 (2013) 240–266.
- [29] M. Singh, S.K. Singh, Anticancer Agents Med. Chem. 14 (2014) 127–146.
- [30] T.D. Bradshaw, A.D. Westwell, Curr. Med. Chem. 11 (2004) 1009–1021.
- [31] G. Akalin Çiftçi, Ş. Ulusoylar Yıldırım, M.D. Altıntop, Z.A. Kaplancıklı, Med. Chem. Res. 23 (2014) 3353–3362.
- [32] H. Wang, N. Zhai, Y. Chen, H. Xu, K. Huang, J. Inorg. Biochem. 172 (2017) 16–22.
- [33] Z. Jin, W.S. El-Deiry, Cancer Biol. Ther. 4 (2005) 139–163.

- [34] J.R. Bencsik, D. Xiao, J.F. Blake, N.C. Kallan, I.S. Mitchell, K.L. Spencer, R. Xu, S.L. Gloor, M. Martinson, T. Risom, R.D. Woessner, F. Dizon, W.I. Wu, G.P. Vigers, B.J. Brandhuber, N.J. Skelton, W.W. Prior, L.J. Murray, *Bioorg. Med. Chem. Lett.* 20 (2010) 7037–7041.
- [35] J. Farand, N. Mai, J. Chandrasekhar, Z.E. Newby, J. Van Veldhuizen, J. Loyer-Drew, C. Venkataramani, J. Guerrero, A. Kwok, N. Li, Y. Zhrebina, S. Wilbert, J. Zablocki, G. Phillips, W.J. Watkins, R. Mourey, G.T. Notte, *Bioorg. Med. Chem. Lett.* 26 (2016) 5926–5930.
- [36] J. Walters, J.L. Schipper, P. Swartz, C. Mattos, A.C. Clark, *Biosci. Rep.* 32 (2012) 401–411.
- [37] C. Cade, P. Swartz, S.H. MacKenzie, A.C. Clark, *Biochemistry* 53 (2014) 7582–7595.
- [38] <http://www.molinspiration.com>. (Accessed August 2017).
- [39] C.A. Lipinski, F. Lombardo, B.W. Dominy, P.J. Feeney, *Adv. Drug Deliv. Rev.* 46 (2001) 3–26.
- [40] D.F. Veber, S.R. Johnson, H.-Y. Cheng, B.R. Smith, K.W. Ward, K.D. Kopple, *J. Med. Chem.* 45 (2002) 2615–2623.
- [41] M.T. Gabr, N.S. El-Gohary, E.R. El-Bendary, M.M. El-Kerdawy, N. Ni, *Chinese Chem. Lett.* 27 (2016) 380–386.
- [42] G. Turan-Zitouni, Z.A. Kaplancikli, K. Erol, F.S. Kiliç, *Farmaco* 54 (1999) 218–223.
- [43] M.D. Altıntop, Z.A. Kaplancikli, G. Turan-Zitouni, A. Özdemir, F. Demirci, G. Iscan, G. Revial, *Synthetic Commun.* 41 (2011) 2234–2250.
- [44] T. Mosmann, *J. Immunol. Methods* 65 (1983) 55–63.
- [45] M.D. Altıntop, H.E. Temel, B. Sever, G. Akalın Çiftçi, Z.A. Kaplancikli, *Molecules* 21 (2016) 1598.
- [46] H.-Y. Zhou, F.-Q. Dong, X.-L. Du, Z.-K. Zhou, H.-R. Huo, W.-H. Wang, H.-D. Zhan, Y.-F. Dai, J. Meng, Y.-P. Sui, J. Li, F. Sui, Y.-H. Zhai, *Bioorg. Med. Chem. Lett.* 26 (2016) 3876–3880.

Table 1. IC₅₀ values of the compounds against A549, C6 and NIH/3T3 cells for 24 h.

Compound	IC ₅₀ (μM)		
	C6 cell line	A549 cell line	NIH/3T3 cell line
1	153.33±35.12	246.67±50.33	96.67±12.58
2	89.33±14.47	91.67±7.64	291.67±59.23
3	236.67±23.10	263.33±47.36	246.67±50.58
4	98.33±12.58	233.33±20.82	335.67±74.54
5	108.33±16.07	210.00±10.00	>403.00
6	4.63±0.85	39.33±4.04	94.33±7.51
7	93.33±15.27	283.33±15.28	>403.00
8	213.33±35.12	228.33±44.81	>403.00
9	66.67±12.58	115.00±5.00	>403.00
Cisplatin	40.67±3.79	70.67±1.15	>403.00
GSK690693	14.5±3.54	105.33±5.03	ND

ND: Not Determined.

Table 2. SI values of the compounds.

Compound	SI values*	
	C6 cell line	A549 cell line
1	0.63	0.39
2	3.27	3.18
3	1.04	0.94
4	3.41	1.44
5	3.72	1.92
6	20.37	2.40
7	4.32	1.42
8	1.89	1.76
9	6.04	3.50
Cisplatin	9.91	5.70

* SI= IC_{50} for normal cell line / IC_{50} for cancerous cell line. $IC_{50} > 403.00$ was accepted as 403.00.

Table 3. Percents of typical quadrant analysis of annexin V-FITC/propidium iodide flow cytometry of C6 and A549 cells treated with the compounds.

Groups	C6 cell line		A549 cell line	
	Early and late apoptotic cells %	Viability %	Early and late apoptotic cells %	Viability %
Control	8.0	90.0	7.1	89.0
Compound 2 treated cells	11.9	84.9	17.0	79.1
Compound 6 treated cells	5.0	92.3	12.2	71.7
Compound 9 treated cells	12.3	80.8	25.3	67.8
Cisplatin treated cells	11.4	81.7	17.8	78.6

C6 and A549 cells were cultured for 24 h in medium with IC_{50} values of compounds. At least 10.000 cells were analyzed per sample, and quadrant analysis was performed.

Table 4. The effects of the compounds on mitochondrial membrane potential of C6 and A549 cells for 24 h.

	C6 cell line		A549 cell line	
	P2 (%)	P3 (%)	P4 (%)	P5 (%)
Control	80.0	19.9	90.4	9.8
Compound 2 treated cells	32.6	60.1	78.2	21.0
Compound 6 treated cells	24.4	74.4	69.8	27.9
Compound 9 treated cells	0.6	98.0	2.4	95.5
Cisplatin treated cells	45.1	55.0	90.0	10.0

Table 5. Percents of typical quadrant analysis of caspase-3 positive/negative C6 and A549 cells treated with the compounds.

Groups	C6 cell line		A549 cell line	
	Caspase-3 (-) cells %	Caspase-3 (+) cells %	Caspase-3 (-) cells %	Caspase-3 (+) cells %
Control	96.4	4.8	98.1	2.1
Compound 2 treated cells	90.8	11.7	93.5	7.1
Compound 6 treated cells	69.8	33.9	76.4	25.0
Compound 9 treated cells	90.1	11.3	95.1	5.4
Cisplatin treated cells	91.6	9.6	90.4	10.5

C6 and A549 cells were cultured for 24 h in medium with IC₅₀ values of compounds. At least 10.000 cells were analyzed per sample, and quadrant analysis was performed.

Table 6. Akt inhibitory effects of the compounds.

Compound	IC ₅₀ (μM)	
	C6 cell line	A549 cell line
2	165.00±5.00	98.33±2.89
6	2.60±0.17	27.50±0.71
9	44.50±3.53	138.33±45.37
Cisplatin	39.00±1.41	34.00±1.73
GSK690693	6.97±0.06	17.33±2.87

Table 7. IC₅₀ values of compounds **2**, **6**, **9** and cisplatin against FAK (Phospho-Tyr397).

Compound	IC ₅₀ (μM)
2	117.50±3.54
6	19.50±2.12
9	105.00±7.07
Cisplatin	59.00±1.41

Table 8. Docking score (kcal/mol), glide gscore (kcal/mol) and glide emodel (kcal/mol) results of compound **6** in the active sites of Akt (PDB code: 3OW4), FAK (PDB code: 5TO8) and caspase-3 (PDB codes: 4EHA and 4QTX).

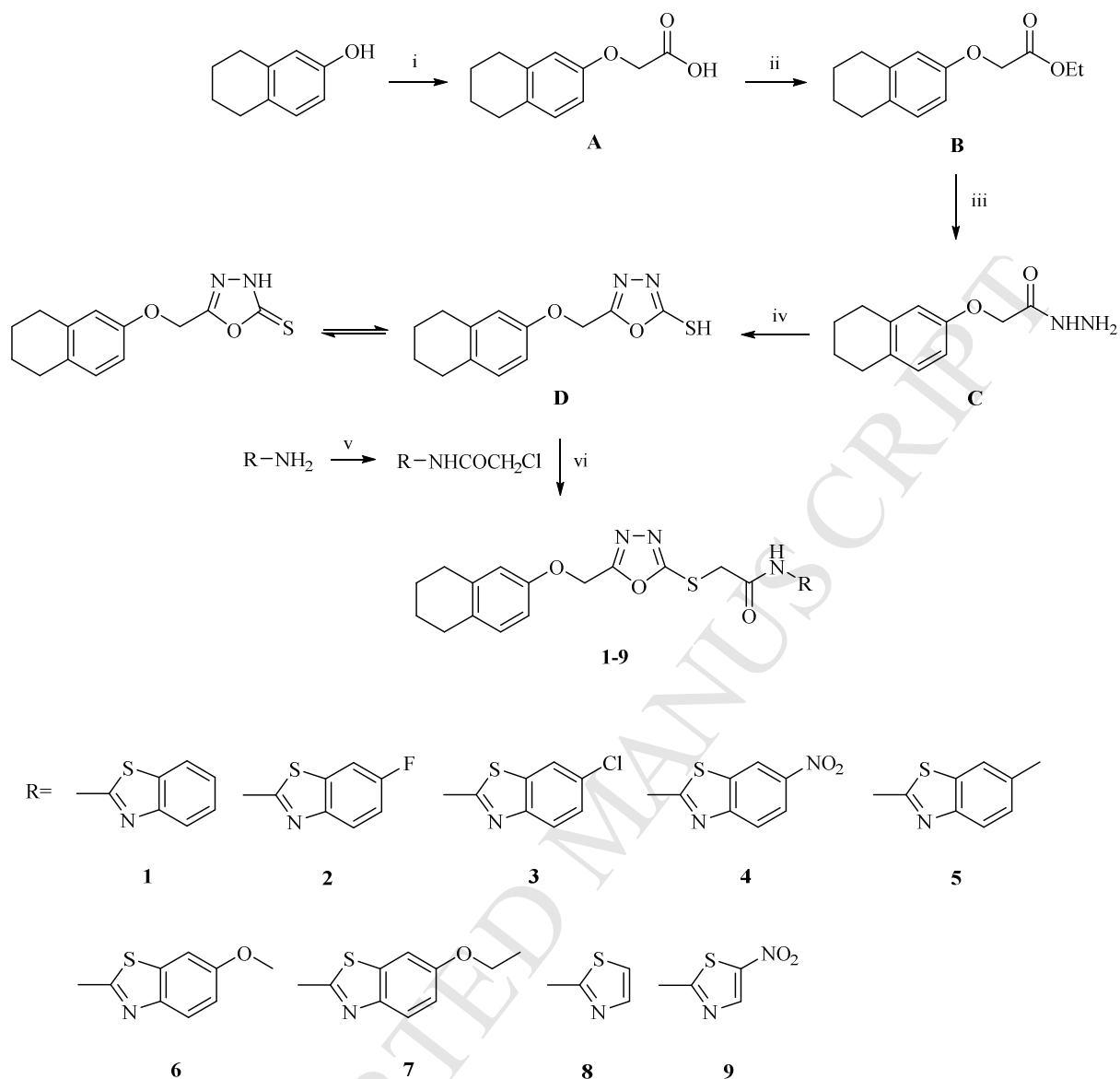
Compound	Enzyme											
	3OW4			5TO8			4EHA			4QTX		
	Docking score	Glide gscore	Glide emodel	Docking score	Glide gscore	Glide emodel	Docking score	Glide gscore	Glide emodel	Docking score	Glide gscore	Glide emodel
6	-6.20	-6.23	-70.25	-3.03	-4.93	-60.73	-1.67	-3.57	-61.32	-2.06	-3.96	-56.85
GSK690693	-6.72	-6.72	-87.38	ND	ND	ND	ND	ND	ND	ND	ND	ND

ND: Not determined.

Table 9. Pharmacokinetic parameters important for bioavailability of compounds **1-9**.

Compound	Molecular properties ^a							
	MW	logP	TPSA	nrotb	HBA	HBD	Volume	Violations
1	452.56	4.36	90.15	7	7	1	379.13	0
2	470.55	4.50	90.15	7	7	1	384.06	0
3	487.01	5.01	90.15	7	7	1	392.67	1
4	497.56	4.29	135.97	8	10	1	402.46	0
5	466.59	4.78	90.15	7	7	1	395.69	0
6	482.59	4.39	99.38	8	8	1	404.68	0
7	496.61	4.77	99.38	9	8	1	421.48	0
8	402.50	2.86	90.15	7	7	1	335.14	0
9	447.50	2.94	135.97	8	10	1	358.47	0

^a Molecular properties were calculated using Molinspiration software. MW: Molecular weight; logP: The logarithm of octanol/water partition coefficient, TPSA: Topological polar surface area; nrotb: Number of rotatable bonds, HBA: Number of hydrogen bond acceptors, HBD: Number of hydrogen bond donors.



Scheme 1. The synthetic route for the preparation of 1,3,4-oxadiazole derivatives (**1-9**). Reagents and conditions: (i) (1) ClCH_2COOH , NaOH , H_2O , reflux, 6 h; (2) H_2SO_4 ; (ii) ethanol, H_2SO_4 , reflux, 6 h; (iii) $\text{NH}_2\text{NH}_2 \cdot \text{H}_2\text{O}$, ethanol, reflux, 2 h; (iv) (1) CS_2 , KOH , ethanol, reflux, 6 h; (2) HCl ; (v) ClCOCH_2Cl , TEA , toluene, 0-5 °C; (vi) K_2CO_3 , acetone, rt, 8 h.

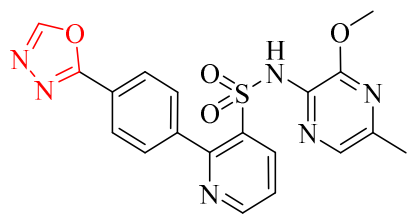
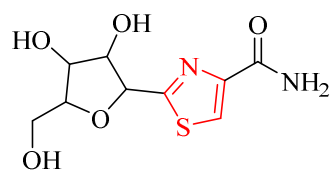
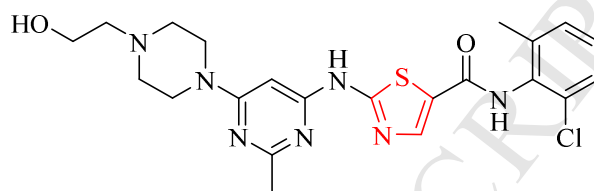


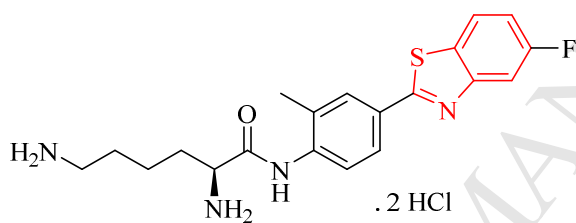
Figure 1. Zibotentan



Tiazofurin



Dasatinib



Phortress

Figure 2. Thiazole and benzothiazole-based anticancer agents

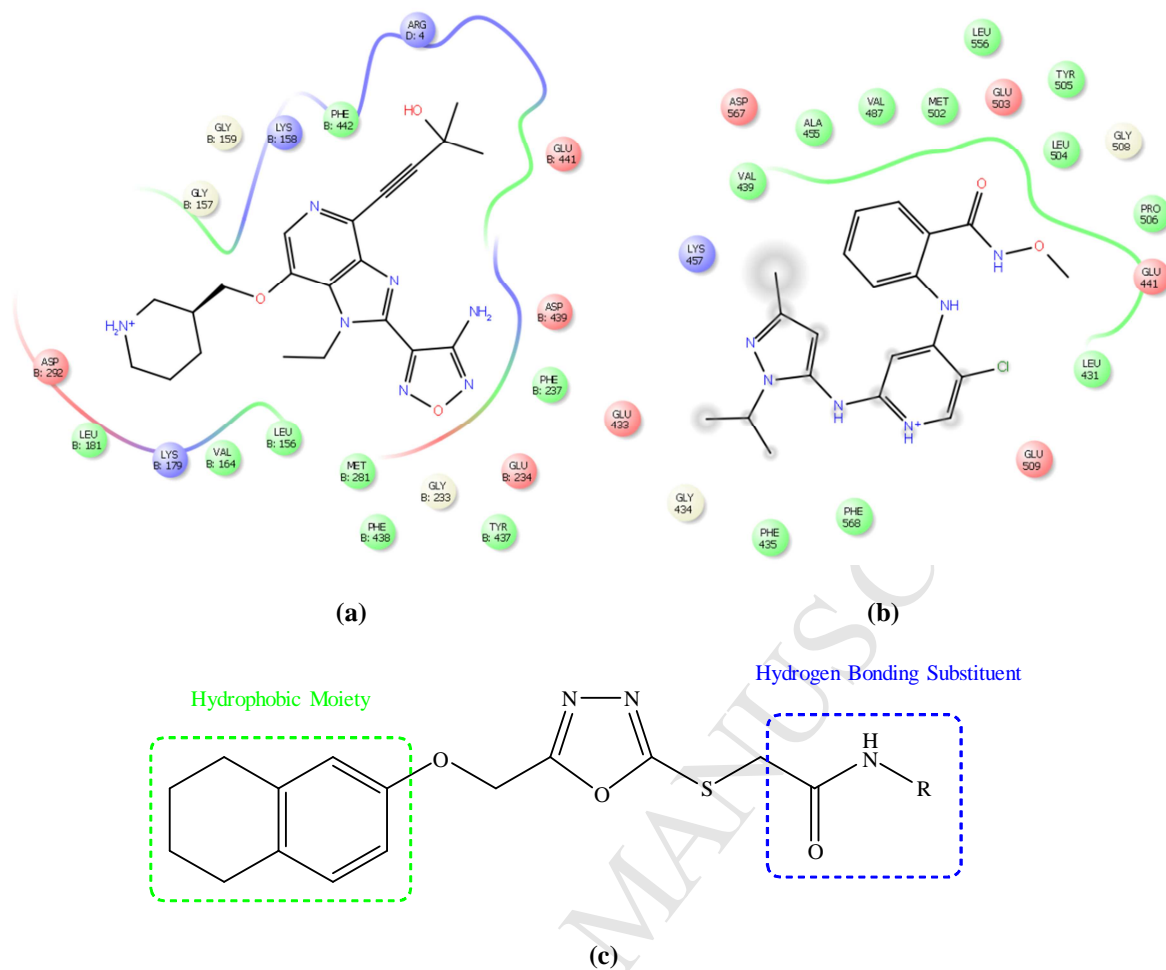


Figure 3. Interactions of GSK690693, a potent pan-AKT kinase inhibitor (a) and GSK2256098, a potent FAK inhibitor (b) with proper residues in the substrate binding site of Akt and FAK, respectively (PDB codes: 3OW4 and 5TO8) (c) Design of 1,3,4-oxadiazole-based inhibitors.

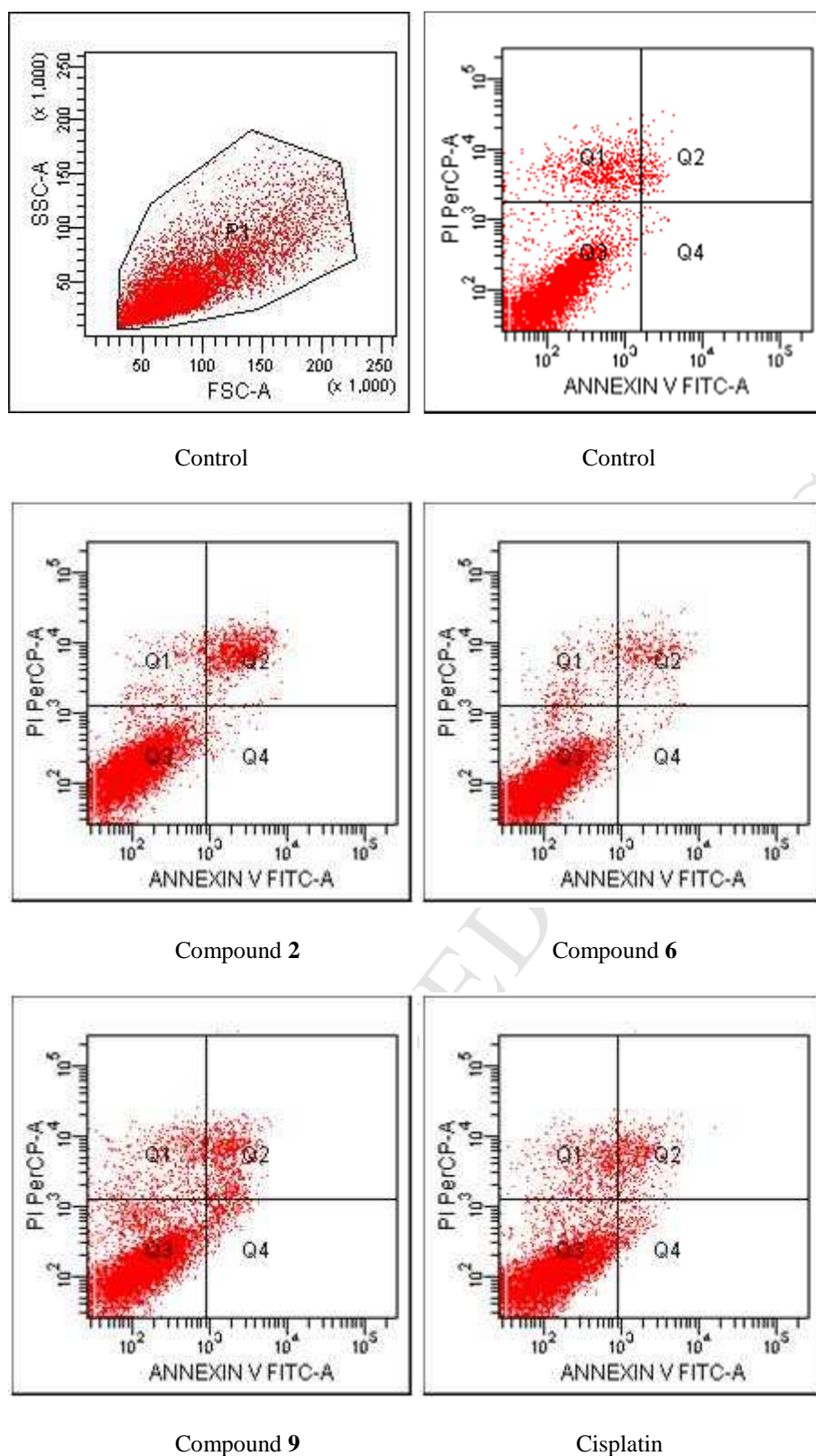


Figure 4. Flow cytometric analysis of C6 cells treated with IC₅₀ values of compounds **2**, **6**, **9** and cisplatin. C6 cells were cultured for 24 h in medium with IC₅₀ values of the compounds. At least 10,000 cells were analyzed per sample, and quadrant analysis was performed.

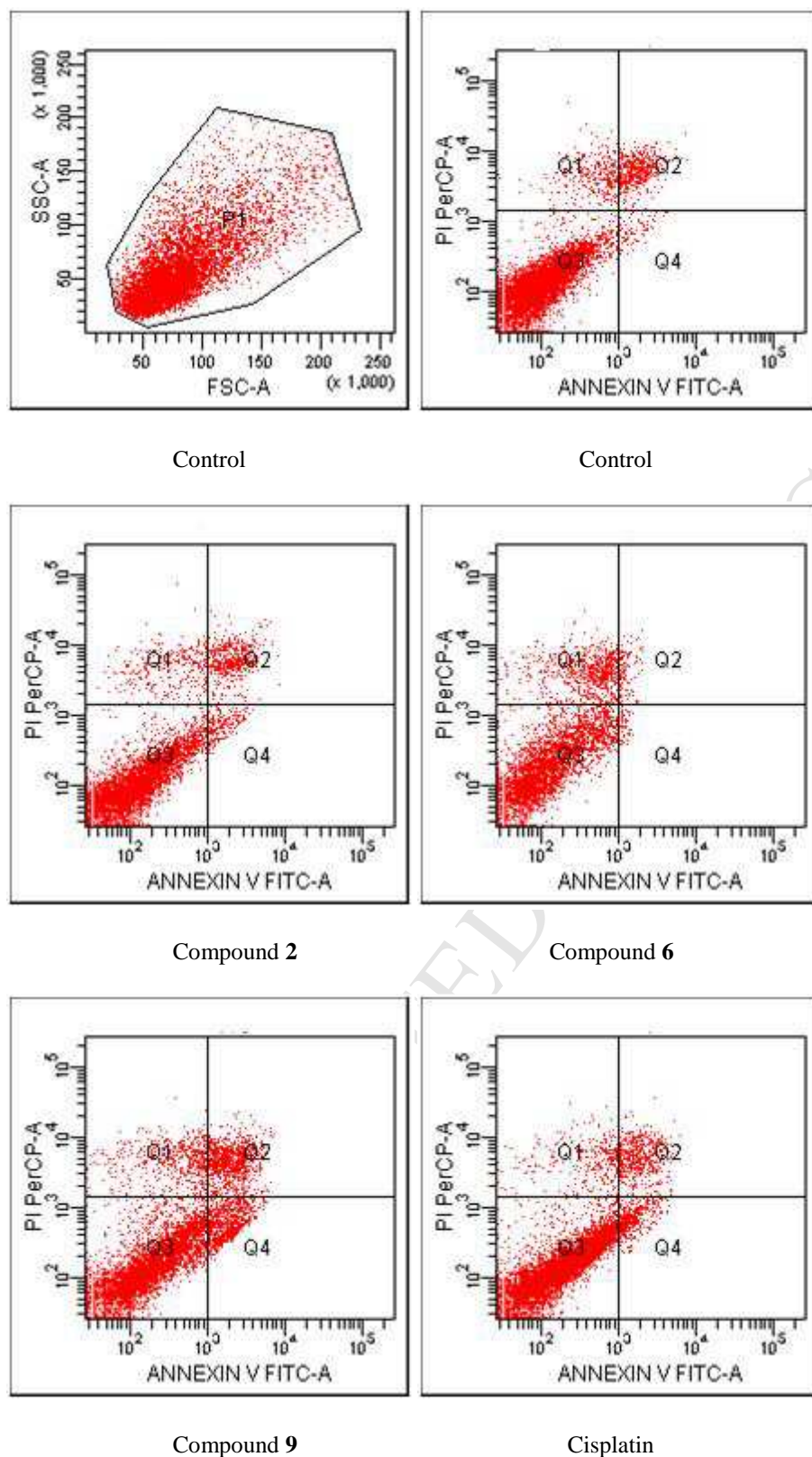


Figure 5. Flow cytometric analysis of A549 cells treated with IC₅₀ values of compounds 2, 6, 9 and cisplatin. A549 cells were cultured for 24 h in medium with IC₅₀ values of the compounds. At least 10,000 cells were analyzed per sample, and quadrant analysis was performed.

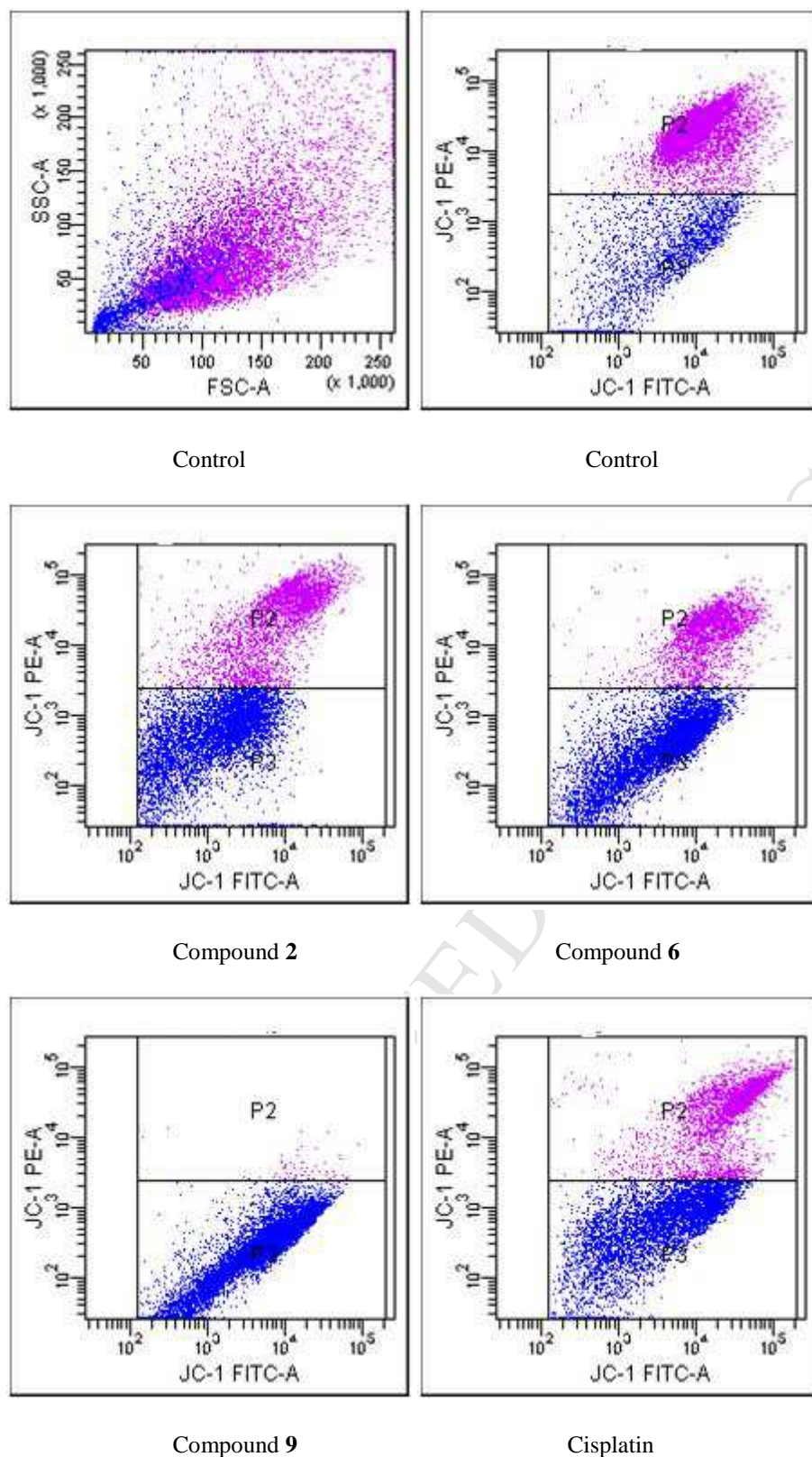


Figure 6. The reduction of the mitochondrial membrane potential in C6 cell line by the compounds. The cells treated or untreated with the IC₅₀ doses of the compounds for 24 h were stained with the mitochondrial-selective JC-1 dye and analyzed by flow cytometry. P2: mitochondrial membrane polarized cells, P3: mitochondrial membrane depolarized cells.

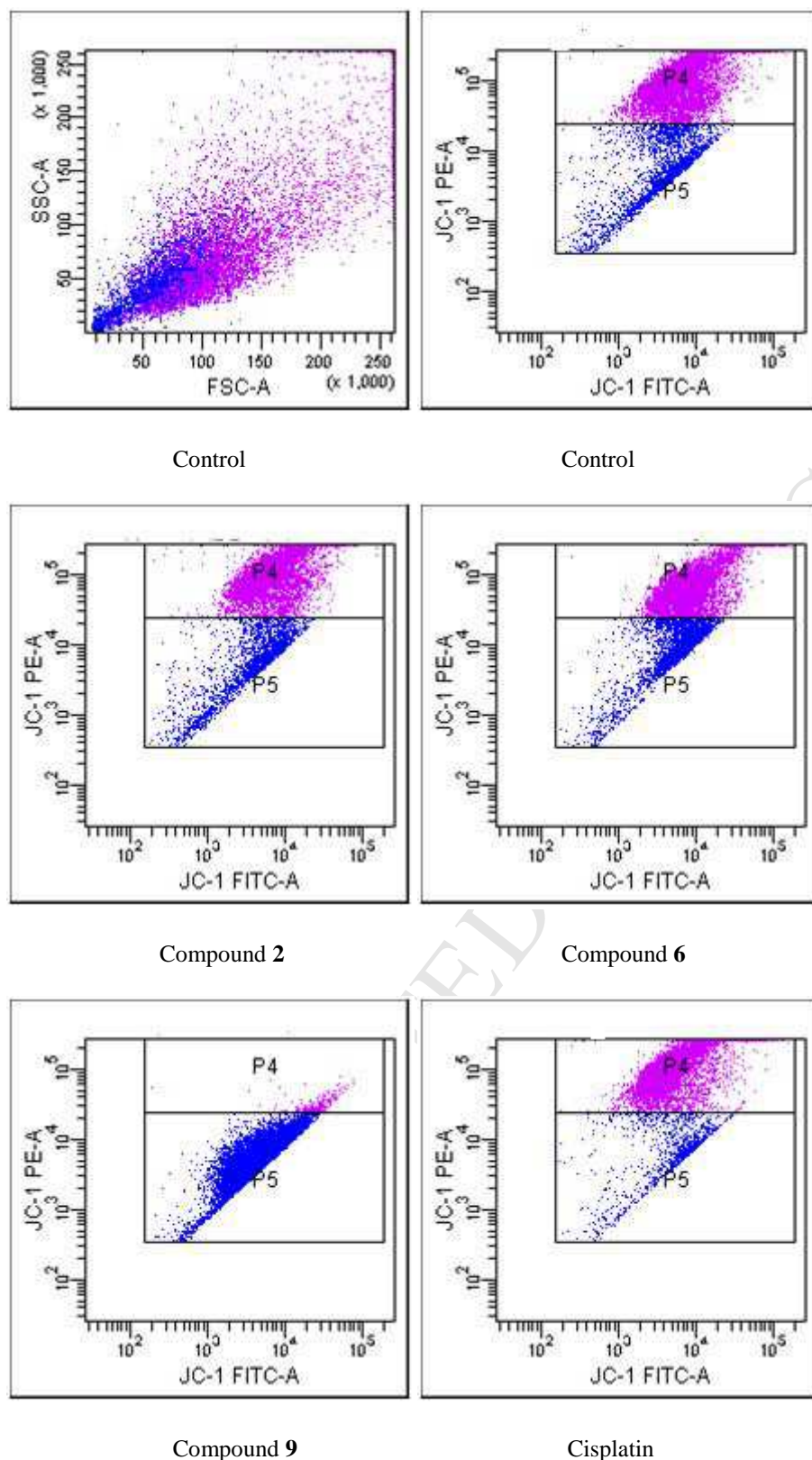


Figure 7. The reduction of the mitochondrial membrane potential in A549 cell line by the compounds. The cells treated or untreated with the IC₅₀ doses of the compounds for 24 h were stained with the mitochondrial-selective JC-1 dye and analyzed by flow cytometry. P4: mitochondrial membrane polarized cells, P5: mitochondrial membrane depolarized cells.

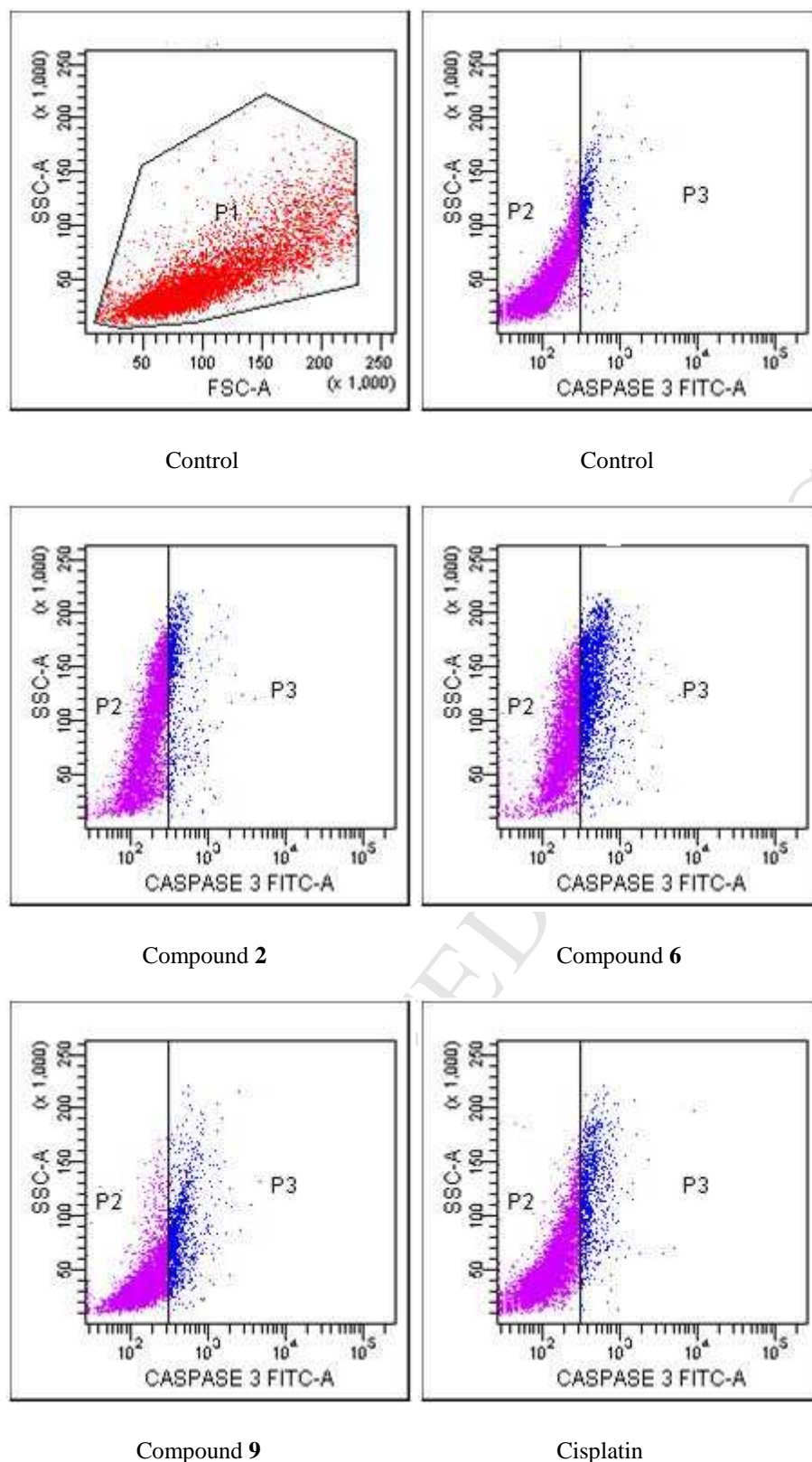


Figure 8. Flow cytometric analysis of Caspase-3 activity in C6 cells treated with IC₅₀ values of compounds **2**, **6**, **9** and cisplatin. C6 glioma cells were cultured for 24 h in medium with IC₅₀ values of the compounds. At least 10,000 cells were analyzed per sample, and quadrant analysis was performed. P2: Caspase 3 (-) cells, P3: Caspase 3 (+) cells.

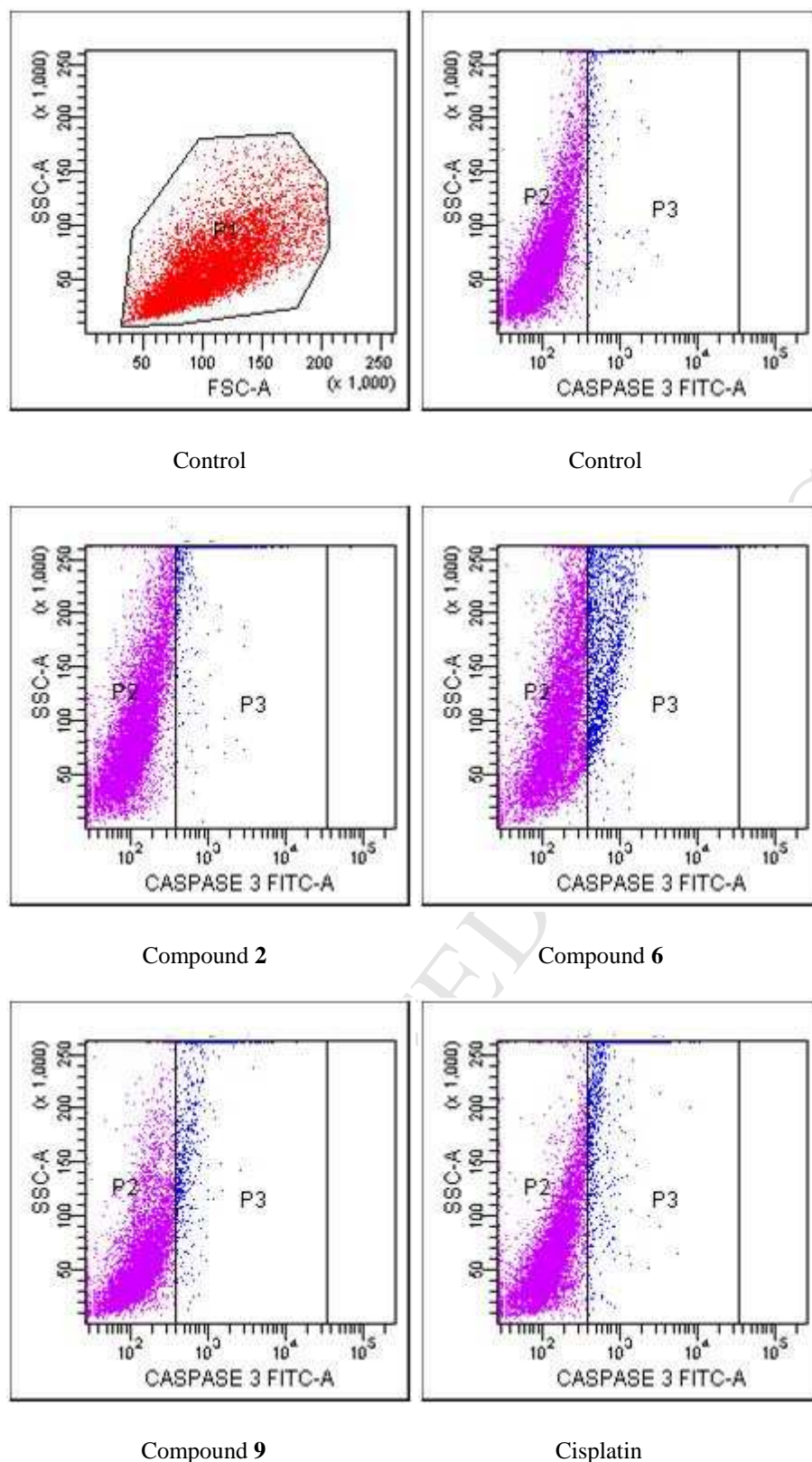


Figure 9. Flow cytometric analysis of Caspase-3 activity in A549 cells treated with IC₅₀ values of compounds **2**, **6**, **9** and cisplatin. A549 cells were cultured for 24 h in medium with IC₅₀ values of the compounds. At least 10,000 cells were analyzed per sample, and quadrant analysis was performed. P2: Caspase 3 (-) cells, P3: Caspase 3 (+) cells.

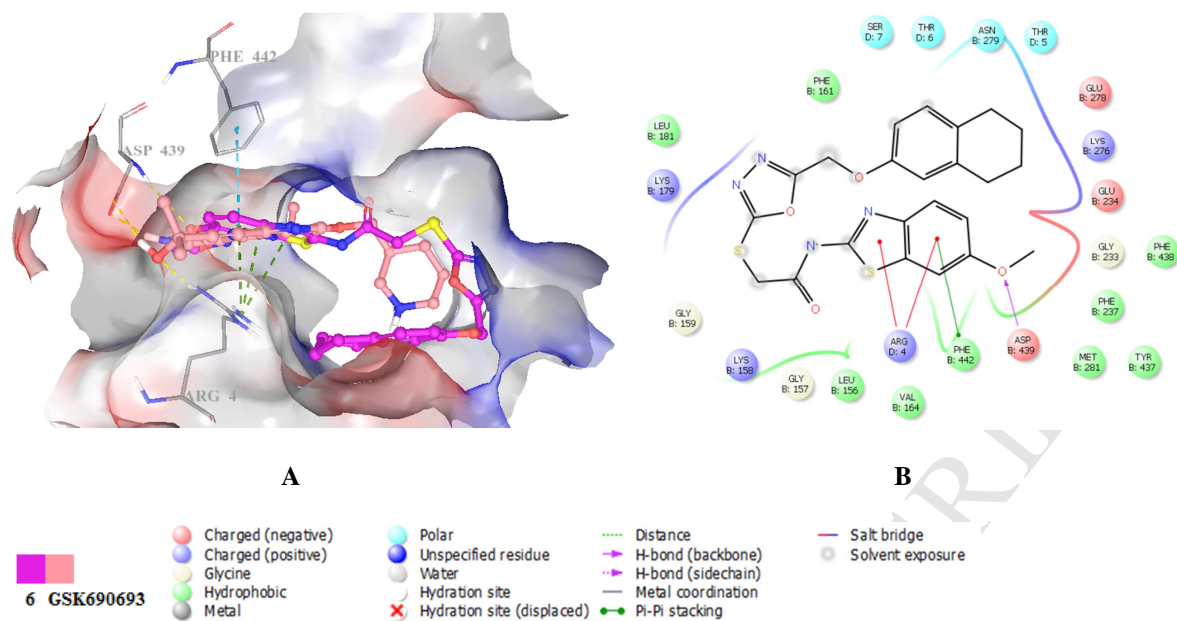


Figure 10. Docking pose (A) and interactions (B) of compound **6** with GSK690693 in the active site of Akt (PDB code: 3OW4).

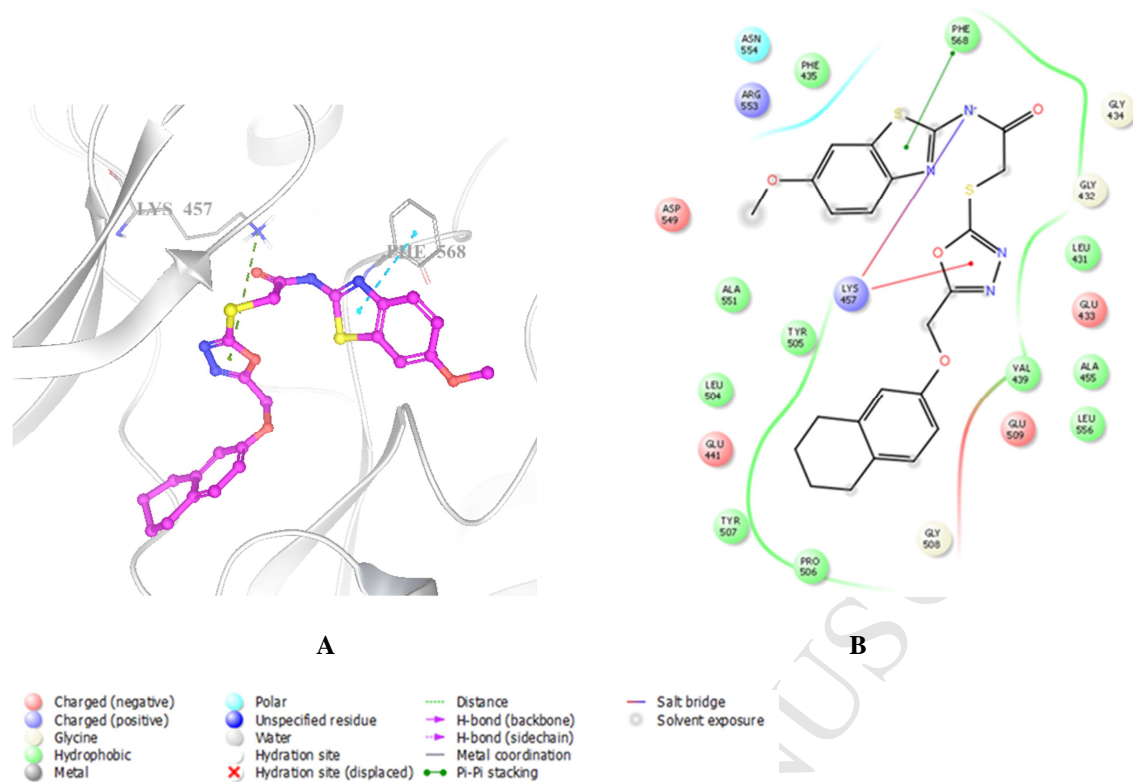


Figure 11. Docking pose (A) and interactions (B) of compound 6 in the active site of FAK (PDB code: 5TO8).

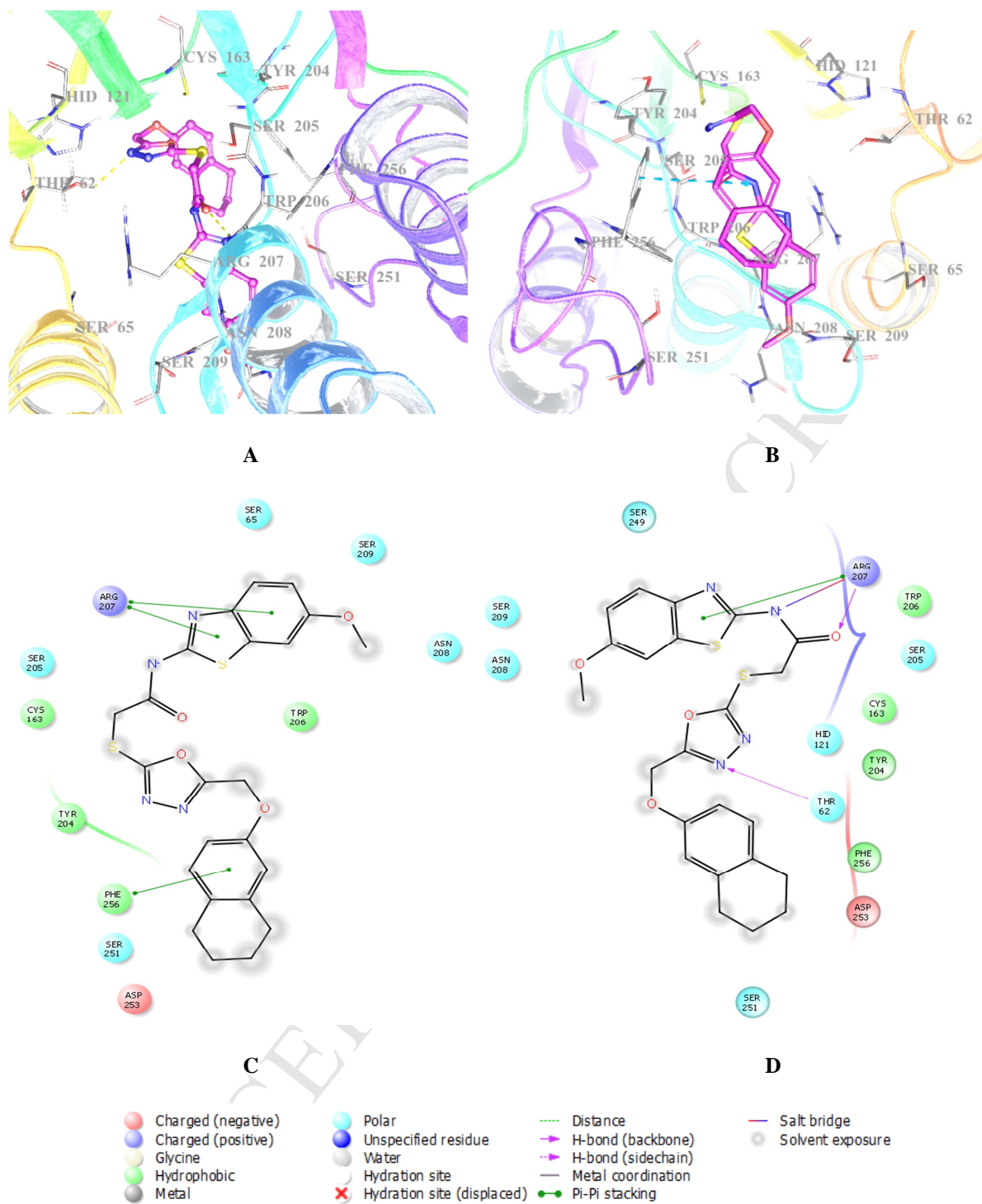
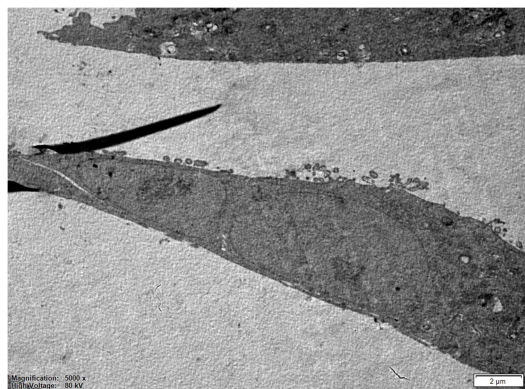
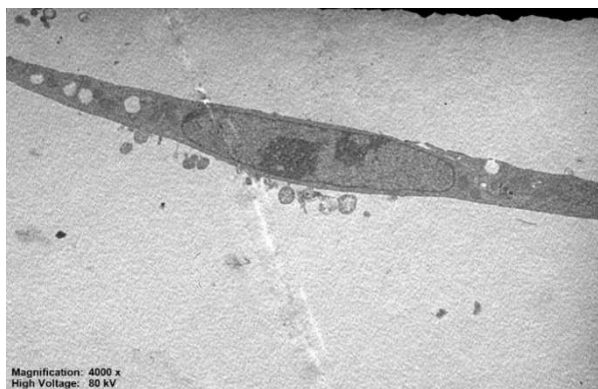


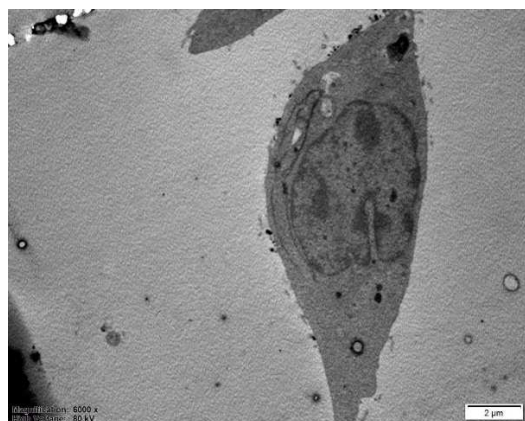
Figure 12. Docking poses and interactions of compound **6** in the active site of caspase-3 (PDB codes: 4EHA (A, C); 4QTX (B, D), respectively).



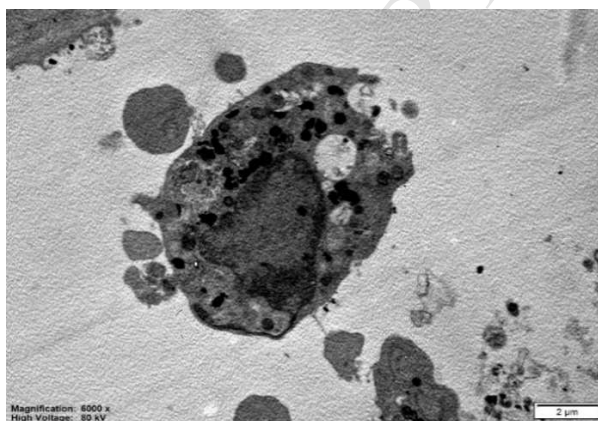
a. Control



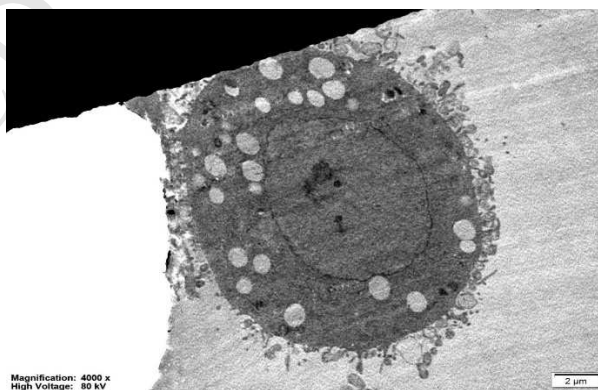
b. Compound 2



c. Compound 6

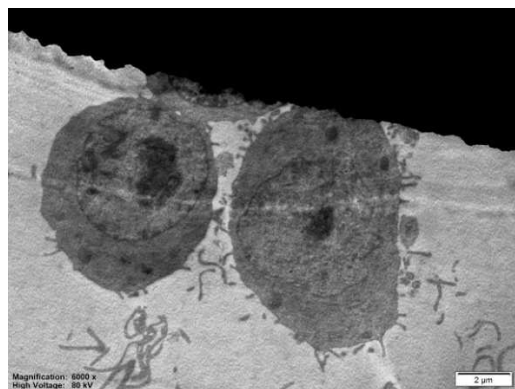


d. Compound 9

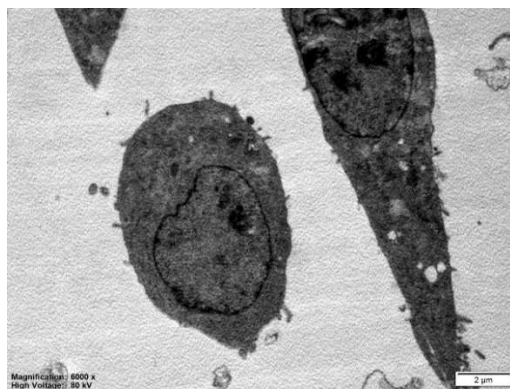


e. Cisplatin

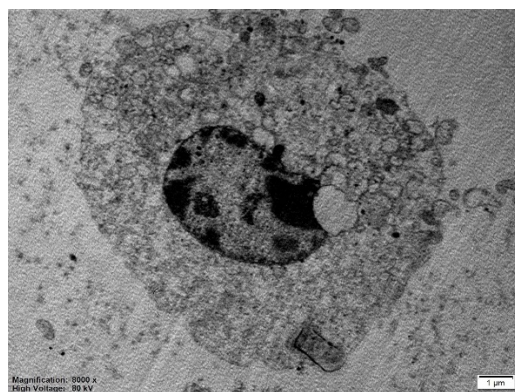
Figure 13. Morphological changes of A549 cells treated with IC_{50} concentrations of compounds 2, 6, 9 and cisplatin for 24 h. a. Control (scale: 2 μ m); b. Compound 2 treated cells (scale: 2 μ m); c. Compound 6 treated cells (scale: 2 μ m); d. Compound 9 treated cells (scale: 2 μ m); e. Cisplatin treated cells (scale: 2 μ m). The shape of the treated cells became round, the cellular organization was disrupted, cell shrinkage and DNA condensation were observed and the membranes of organelles were sharply damaged.



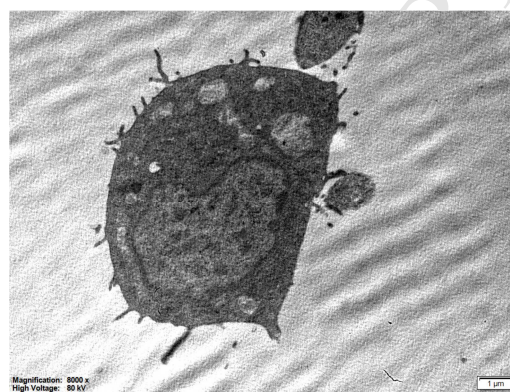
a. Control



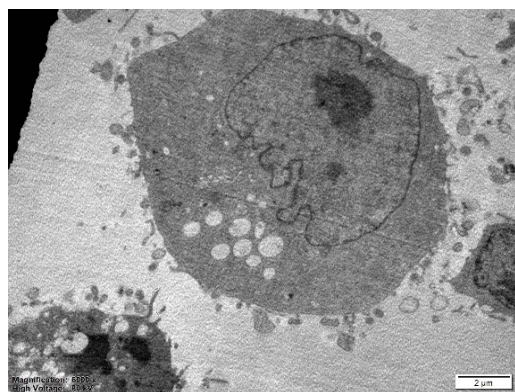
b. Compound 2



c. Compound 6



d. Compound 9



e. Cisplatin

Figure 14. Morphological changes of C6 cells treated with IC_{50} concentrations of compounds **2**, **6**, **9** and cisplatin for 24 h. a. Control (scale: 2 μ m); b. Compound **2** treated cells (scale: 2 μ m); c. Compound **6** treated cells (scale: 2 μ m); d. Compound **9** treated cells (scale: 2 μ m); e. Cisplatin treated cells (scale: 2 μ m). The shape of the treated cells became round, the cellular organization was disrupted, cell shrinkage and DNA condensation were observed and the membranes of organelles were sharply damaged.

Highlights

- ▶ Compounds **2**, **6** and **9** were identified as potent oxadiazole-based anticancer agents.
- ▶ Compound **6** was found to be a potent Akt inhibitor.
- ▶ Compound **6** showed significant FAK inhibitory activity.
- ▶ Compound **6** caused higher caspase-3 activation than cisplatin in both cell lines.
- ▶ According to *in silico* studies, they were expected to have good oral bioavailability.